Modeling Nonlinear Systems by Volterra Series

Luigi Carassale, M.ASCE[1]; and Ahsan Kareem, Dist.M.ASCE[2]

Abstract: The Volterra-series expansion is widely employed to represent the input-output relationship of nonlinear dynamical systems. This representation is based on the Volterra frequency-response functions (VFRFs), which can either be estimated from observed data or through a nonlinear governing equation, when the Volterra series is used to approximate an analytical model. In the latter case, the VFRFs are usually evaluated by the so-called harmonic probing method. This operation is quite straightforward for simple systems but may reach a level of such complexity, especially when dealing with high-order nonlinear systems or calculating high-order VFRFs, that it may loose its attractiveness. An alternative technique for the evaluation of VFRFs is presented here with the goal of simplifying and possibly automating the evaluation process. This scheme is based on first representing the given system by an assemblage of simple operators for which VFRFs are readily available, and subsequently constructing VFRFs of the target composite system by using appropriate assemblage rules. Examples of wind and wave-excited structures are employed to demonstrate the effectiveness of the proposed technique.

DOI: 10.1061/(ASCE)EM.1943-7889.0000113

CE Database subject headings: Nonlinear systems; Stochastic processes.

Author keywords: Nonlinear dynamics; Volterra series; Stochastic response.

Introduction

The Volterra series is a mathematical tool widely employed for representing the input-output relationship of nonlinear dynamical systems (Volterra 2005). It is akin to the Taylor series but with memory, whereas the Taylor series is a static expansion in nature. It is based on the expansion of the nonlinear operator representing the system into a series of homogeneous operators, formally similar to the Duhamel integral usually employed for the analysis of linear systems. These integral relationships are multidimensional and are completely defined by the Volterra kernels, i.e., the multidimensional generalization of the impulse-response function (Schetzen 1980). An alternative representation is provided by the Volterra frequency-response functions (VFRFs), which represent the frequency-domain counterparts of the Volterra kernels and can be reviewed as a generalization of the usual frequency-response function for nonlinear systems where the linear system is a special case. A fairly large class of dynamical systems can be treated according to these concepts and are accordingly represented in terms of VFRFs.

Applications of the Volterra series are widespread in several fields of engineering and physics and can be roughly classified into two distinct categories. In the first, the Volterra series is used to build a model of an observed dynamical phenomenon and the VFRFs are estimated from experimental or numerically generated data. This "computationally thinking" approach represents "data to knowledge" as it is applied with the aim of realizing mathematical models that capture observed physical behaviors [e.g., Koukoulas et al. (1995) and Silva (2005)] or to construct reduced-order models that can reproduce selected features of a complex numerical model [e.g., Lucia et al. (2004)]. In this context, the modeling of wave-induced forces on large floating offshore structures often utilizes this approach in which the output of Volterra systems of second or third order is used to represent hydrodynamic loads based on the diffraction theory [e.g., Chakrabarti (1990), Donley and Spanos (1991), Kareem and Li (1994) and Kareem et al. (1994, 1995)].

The second of the two mentioned classes of applications concerns the analysis of dynamical systems that are already represented by an analytical model, for example, a differential equation. In this case, the Volterra-series representation has been successfully used to investigate the behavior of harmonically excited nonlinear systems [e.g., Worden and Manson (2005)] or to calculate the probabilistic response of randomly excited systems [e.g., Donley and Spanos (1990), Spanos and Donley (1991, 1992), Kareem et al. (1995), and Tognarelli et al. (1997a,b)].

When an analytical model of the dynamical system is available, the VFRFs are usually calculated by means of the harmonic probing approach, which consists of evaluating analytically the response of the system excited by products of harmonic functions with different frequencies (Bedrosian and Rice 1971). As discussed by Peyton Jones (2007), this operation is quite straightforward for simple systems, but may reach a high level of computational complexity when dealing with high-order nonlinear systems or for the calculation of high-order VFRFs.

A new alternative technique is presented here with the aim of simplifying the evaluation of the VFRFs of dynamical systems represented by analytical models and to enable the analysis of systems realized by combining analytical models and Volterra systems based on numerical or experimental approaches. This method involves representing a complex dynamical system by an assemblage of simple operators for which VFRFs are readily

[1]Assistant Professor of Engineering, Dept. of Civil Environmental and Architectural Engineering, Univ. of Genova, 16145 Genova, Italy (corresponding author). E-mail: luigi.carassale@unige.it

[2]Robert M. Moran Professor of Engineering, NatHaz Modelling Laboratory, Univ. of Notre Dame, IN 46556.

Note. This manuscript was submitted on May 18, 2009; approved on November 5, 2009; published online on November 6, 2009. Discussion period open until November 1, 2010; separate discussions must be submitted for individual papers. This paper is part of the ***Journal of Engineering Mechanics***, Vol. 136, No. 6, June 1, 2010. ©ASCE, ISSN 0733-9399/2010/6-801–818/$25.00.

available (Carassale and Karrem 2003). The topology of the assemblage is determined by the physical nature of the system or by the mathematical structure of the governing equation. Accordingly, this paper provides the VFRFs of some simple dynamical systems and presents a set of rules for the evaluation of the VFRFs of the composites representing the target. This approach formally simplifies the computation of VFRFs and enables the use of symbolic manipulation software. The proposed assemblage rules are used to derive explicit expressions for the statistical moments of the response of a Volterra system excited by a Gaussian stationary random process.

Five simple examples of waves and wind-excited single degree-of-freedom systems are considered to demonstrate the application of the proposed technique. The probabilistic response in terms of cumulants and power spectral density (PSD) functions is evaluated by employing the frequency-domain approach, which involves integration of the VFRFs and is compared to the results of the time-domain Monte Carlo simulation (MCS) for different orders of truncation of the Volterra series. A further comparison involves the probability density functions (PDFs), estimated by the time-domain MCS and through a translation model based on the first four cumulants obtained by the integration of the VFRFs. To the best of writers' knowledge, it is the first time that the first four cumulants of the response of a dynamical system are estimated by employing a fifth-order Volterra-series expansion. Previous applications were limited to the expansion at the third order due to analytical complications and computational complexity.

Volterra Series: Background and Definitions

Let us consider the nonlinear system represented by the following equation:

$$x(t) = \mathcal{H}[u(t)] \tag{1}$$

where $u(t)$ and $x(t)$=input and the output, respectively, and t=time. If the operator $\mathcal{H}[\cdot]$ is time-invariant and has finite memory, its output $x(t)$ can be expressed, far enough from the initial conditions, through the Volterra-series expansion [e.g., Schetzen (1980)]

$$x(t) = \sum_{j=0}^{\infty} x_j(t) = \sum_{j=0}^{\infty} \mathcal{H}_j[u(t)] \tag{2}$$

in which each term x_j is the output of an operator $\mathcal{H}_j$, homogeneous of degree j, referred to as the jth order Volterra operator. The zeroth-order term $x_0=\mathcal{H}_0$ is a constant output independent of the input, while the generic jth-order term ($j \geq 1$) is given by the expression

$$\mathcal{H}_j[u(t)] = \int_{\boldsymbol{\tau}_j \in \mathbb{R}^j} h_j(\boldsymbol{\tau}_j) \prod_{r=1}^{j} u(t-\tau_r) d\boldsymbol{\tau}_j \quad (j = 1,2,\ldots) \tag{3}$$

where $\boldsymbol{\tau}_j=[\tau_1,\ldots,\tau_j]^T$ is a vector containing the j integration variables and the functions h_j=Volterra kernels. The first-order term is the convolution integral typical of linear dynamical systems with h_1 being the impulse-response function. The higher-order terms are multiple convolutions, involving products of the input values for different delay times. The expanded version of Eq. (3) up to the order $j=3$ is given in the Appendix [Eq. (82)].

The series defined in Eq. (2) is in principle composed of infinite terms and, for practical applications, needs to be conveniently truncated retaining the terms up to some order n. Within this framework, the operator $\mathcal{H}$ is represented by the parallel assemblage of a finite number $(n+1)$ of Volterra operators $\mathcal{H}_0,\ldots,\mathcal{H}_n$ (Fig. 1) and is referred to as an nth-order Volterra system.

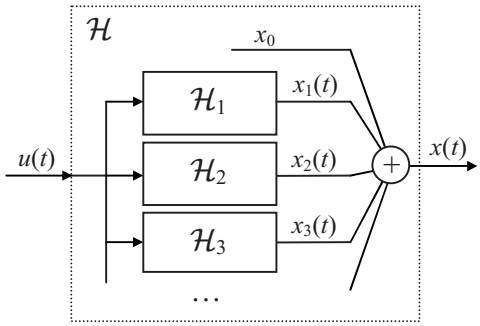

Fig. 1. Block diagram for a Volterra system

The expression of the Volterra operators provided by Eq. (3) can be slightly generalized defining the multilinear operators

$$\mathcal{H}_j\{u_1(t),\ldots,u_j(t)\} = \int_{\boldsymbol{\tau}_j \in \mathbb{R}^j} h_j(\boldsymbol{\tau}_j) \prod_{r=1}^{j} u_r(t-\tau_r) d\boldsymbol{\tau}_j \quad (j = 2,\ldots,n) \tag{4}$$

where $u_1,\ldots,u_j=j$, in general different, scalar inputs. From Eq. (4), it obviously results that $\mathcal{H}_j\{u,\ldots,u\}=\mathcal{H}_j[u]$.

A Volterra system is completely defined by its constant output and its Volterra kernels. An alternative representation in the frequency domain is provided by the VFRF, the multidimensional Fourier transform of the Volterra kernel

$$H_j(\boldsymbol{\Omega}_j) = \int_{\boldsymbol{\tau}_j \in \mathbb{R}^j} e^{-i\boldsymbol{\Omega}_j^T \boldsymbol{\tau}_j} h_j(\boldsymbol{\tau}_j) d\boldsymbol{\tau}_j \quad (j = 1,\ldots,n) \tag{5}$$

where $\boldsymbol{\Omega}_j=[\omega_1\ldots\omega_j]^T$ is a vector containing the j circular frequency values corresponding to $\tau_1,\ldots,\tau_j$ in the Fourier transform pair. For completeness of the notation, the zeroth-order VFRF is defined as the zeroth-order output, i.e., $H_0=x_0$.

The Volterra operators defined by Eq. (3) are not unique and can always be chosen in such a way that the corresponding multilinear operators $\mathcal{H}_j\{u_1,\ldots,u_j\}$ are symmetric (i.e., independent of the ordering of the j inputs). This assumption works as a consequence of symmetry of the Volterra kernels and VFRFs, respectively, as noted in Eqs. (4) and (5) [e.g., Schetzen (1980)]. It follows that any no-symmetric Volterra operator, defined by the VFRF $\tilde{H}_j$, can be replaced by its equivalent symmetric one, whose VFRF is given by

$$H_j(\boldsymbol{\Omega}_j) = \mathrm{sym}[\tilde{H}_j(\boldsymbol{\Omega}_j)] = \frac{1}{j!} \sum_{\substack{\text{all } j\text{th-order} \\ \text{permuting} \\ \text{matrices } \mathbf{E}}} \tilde{H}_j(\mathbf{E}\boldsymbol{\Omega}_j) \tag{6}$$

Frequency-Domain Response of Volterra Systems

The response $x(t)$ of the Volterra system $\mathcal{H}$ can be calculated through the time-domain integrals given by Eq. (3), but alternative relationships based on the VFRFs are often preferred. In order to find such relationships, including the treatment of both

deterministic and stationary random inputs, the Fourier-Stieltjes representation of the input is considered [e.g., Priestley (1981)]

$$u(t) = \int_{-\infty}^{\infty} e^{i\omega t} dU(\omega) \tag{7}$$

where $U(\omega)$=complex-valued (possibly random) function of ω whose derivative (wherever it exists) is the Fourier transform of u, while its increments $dU(\omega)=U(\omega+d\omega)-U(\omega)$ represent the amplitude (possibly finite) of each harmonic composing u. When u is a stationary random process, $dU(\omega)$ is a random interval function. Besides, it can be shown that if u is zero-mean process and has a finite PSD function, then $dU(\omega)$ has zero mean for $\omega \neq 0$ and satisfies the following relationships:

$$dU^*(-\omega) = dU^*(\omega) \quad \omega \neq 0$$

$$E[dU(\omega)dU^*(\omega')] = \begin{cases} 0 & \text{if } \omega \neq \omega' \\ S_{uu}(\omega)d\omega & \text{if } \omega = \omega' \end{cases} \tag{8}$$

where $E[\cdot]$=statistical expectation operator; the superscript * represents the complex conjugate, and $S_{uu}(\omega)$=PSD of $u(t)$. If the process $u(t)$ is Gaussian, then the increments $dU(\omega)$ are circular-complex Gaussian variables (Amblard et al. 1996) and the following property holds:

$$E\left[\prod_{r=1}^{j} dU(\omega_r)\right] = \frac{j!}{(j/2)!2^{j/2}} \prod_{r=1}^{j/2} S_{uu}(\omega_{2r})\delta(\omega_{2r}+\omega_{2r-1})d\omega_{2r}d\omega_{2r-1} \tag{9}$$

for any even j, while the expectation vanishes for any odd j; δ is the Dirac delta function.

The jth order output of the Volterra operator $\mathcal{H}$ can be obtained by substituting Eq. (7) into Eq. (3), resulting in

$$\mathcal{H}_j[u] = \int_{\boldsymbol{\tau}_j \in \mathbb{R}^j} h_j(\boldsymbol{\tau}_j) \prod_{r=1}^{j} \int_{-\infty}^{\infty} e^{i\omega_r(t-\tau_r)} dU(\omega_r) d\boldsymbol{\tau}_j \quad (j = 1, \ldots, n) \tag{10}$$

or changing the order of integration

$$\mathcal{H}_j[u] = \int_{\boldsymbol{\Omega}_j \in \mathbb{R}^j} e^{i\Sigma\boldsymbol{\Omega}_j t} \int_{\boldsymbol{\tau}_j \in \mathbb{R}^j} e^{-i\boldsymbol{\Omega}_j^T \boldsymbol{\tau}_j} h_j(\boldsymbol{\tau}_j) d\boldsymbol{\tau}_j \prod_{r=1}^{j} dU(\omega_r) \quad (j = 1, \ldots, n) \tag{11}$$

where $\Sigma\boldsymbol{\Omega}_j=\omega_1+\ldots+\omega_j$.

The comparison of Eqs. (5) and (11) provides the final expression for the jth-order Volterra operator

$$\mathcal{H}_j[u] = \int_{\boldsymbol{\Omega}_j \in \mathbb{R}^j} e^{i\Sigma\boldsymbol{\Omega}_j t} H_j(\boldsymbol{\Omega}_j) \prod_{r=1}^{j} dU(\omega_r) \tag{12}$$

Note that Eq. (12) {explicitly reported in the Appendix [Eq. (83)] for $j=1$ to 3} is also valid for the zeroth-order term for which it reduces to $\mathcal{H}_0=H_0$. The outputs x_j of the operators $\mathcal{H}_j$ can be represented by expressions analogous to Eq. (7) in terms of the random interval processes $dX_j(\omega)$, which can be obtained by the relationships

$$dX_0 = H_0\delta(\omega)d\omega$$

$$dX_j(\omega) = \int_{\substack{\boldsymbol{\Omega}_j \in \mathbb{R}^j \\ \Sigma\boldsymbol{\Omega}_j=\omega}} H_j(\boldsymbol{\Omega}_j) \prod_{r=1}^{j} dU(\omega_r) \quad (j = 1, \ldots, n) \tag{13}$$

where the integration in the second equation is performed on the subspace of $\mathbb{R}^j$ with dimension $j-1$, in which the constraint $\Sigma\boldsymbol{\Omega}_j=\omega$ is satisfied. From this equation {expanded for $j=1$ to 3 in the Appendix [Eq. (83)]}, it can be easily noted that the interval processes corresponding to the high-order outputs are provided by the frequency-domain convolutions of the input $dU(\omega)$, allowing the spectral power of the input to spread throughout the output spectrum.

Evaluation of the VFRFs

When an analytical model (e.g., a differential equation) of a dynamical system is available, the VFRFs are traditionally calculated by means of the direct expansion method [i.e., manipulation of the system to recast it in the form of Eqs. (2) and (3)] or by the harmonic probing method (Bedrosian and Rice 1971). The proposed formulation requires the derivation of expressions for the VFRFs of simple systems (FRFs for Simple Systems Section) and the formulation of a set of algebraic rules allowing the construction of any possible topology of the composite combined configuration of Volterra operators (VFRFs Composite Systems: Assemblage Rules Section).

FRFs for Simple Systems

Simple linear systems, such as differential and delay operators, as well as memoryless nonlinear systems are discussed in order to construct a library of building block elementary systems to be used in the subsequent assemblage.

Differential and Integral Operators

Let the operator $\mathcal{H}$ be defined by the differential relationship

$$\mathcal{H}[u] = \frac{d^r u}{dt^r} \tag{14}$$

where r denotes the order of the derivative. Substituting Eq. (7) into Eq. (14) and comparing to Eq. (12), suggests that $H_j=0$ for $j \neq 1$ and

$$H_1(\omega) = (i\omega)^r \tag{15}$$

It can be observed that VFRFs in the form of Eq. (15) can also represent integral operators ($r<0$) and fractional derivatives ($r \in \mathbb{R}$).

Delay Operator

Let $\mathcal{H}$ be a delay operator defined as

$$x(t) = \mathcal{H}[u(t)] = u(t-T) \tag{16}$$

where T is the delay time. It can be shown that $\mathcal{H}$ is a linear operator ($H_j=0$ for $j \neq 1$) and that

$$H_1(\omega) = e^{-i\omega T} \tag{17}$$

Polynomial and Memoryless Nonlinearities

Let the operator $\mathcal{H}$ be expressed by the nth-order polynomial function:

$$\mathcal{H}[u] = \sum_{j=0}^{n} a_j u^j \tag{18}$$

where a_j are constant coefficients. Substituting Eq. (7) into Eq. (18) and comparing to Eq. (12), the VFRFs are readily obtained as

$$H_j(\mathbf{\Omega}_j) = a_j \quad (j = 0, \ldots, n) \tag{19}$$

These VFRFs do not depend on the frequency, reflecting the fact that $\mathcal{H}$ is a memoryless operator.

In the case in which $\mathcal{H}$ is expressed by a generic nonlinear function of the input $\mathcal{H}[u]=g(u)$, a polynomial approximation can be adopted before applying the solution given by Eqs. (18) and (19). For this purpose, different approaches may be applied. The simplest approach consists of expanding the nonlinear function g into a Taylor series to obtain a polynomial expression in u; this method is applicable only if g is differentiable at the mean value of u and may result in an inadequate convergence rate when far from the origin. Similar polynomial expressions can be obtained by minimizing some measure of the error between the actual nonlinearity and the approximating polynomial; a typical choice is the mean-square measure

$$\varepsilon = E\left[\left(g(u) - \sum_{j=0}^{n} a_j u^j\right)^2\right] \tag{20}$$

The polynomial coefficients providing the minimization of ε can be estimated by a linear system involving the statistical moment (and cross moments) of the input u and of the output x (Donley and Spanos 1990, 1991; Spanos and Donley 1991, 1992; Li et al. 1995)

$$\mathbf{Ma} = \mathbf{b} \tag{21}$$

where $\mathbf{a}=[a_0, \ldots, a_n]^T$; $b_j=E[u^j g(u)]$; and $M_{jk}=E[u^{j+k-2}]$ $(j,k=1, \ldots, n+1)$. If the input u is Gaussian and zero mean, then the $j-k$th element of the matrix $\mathbf{M}$ is given by the expression

$$M_{jk} = \begin{cases} \dfrac{(j+k-2)!}{\left(\dfrac{j+k}{2}-1\right)!2^{\left(\frac{j+k}{2}-1\right)}}\sigma_u^{j+k-2} & j+k \text{ even} \\ 0 & j+k \text{ odd} \end{cases}$$
$$(j,k = 1, \ldots, n+1) \tag{22}$$

where σ_u=standard deviation (SD) of the input u.

An alternative method consists of estimating the polynomial coefficients in such a way as to match the first few statistical moments of the actual output; this constraint leads to a set of nonlinear algebraic equations involving the $n+1$ statistical moments m_j of the input and of the output (Winterstein 1988; Kareem et al. 1995).

$$m_j\left[\sum_{k=0}^{n} a_k u^k\right] = m_j[g(u)] \quad (j = 1, \ldots, n+1) \tag{23}$$

The latter approach has been found to be, in some circumstances, more reliable than the former, thanks to its ability of retaining, in the approximation, the exact statistics of the actual nonlinearity.

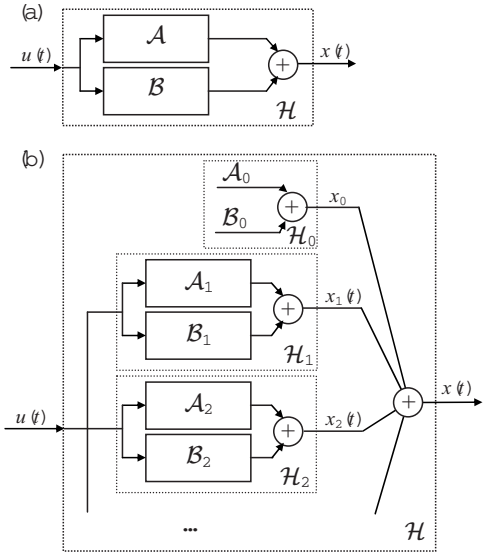

Fig. 2. Block diagram for parallel combination of Volterra systems

Besides, the numerical implementation of this approach is more efficient for non-Gaussian processes (Tognarelli and Kareem 2001).

VFRFs for Composite Systems: Assemblage Rules

Rules for the parallel and series combination of Volterra systems, as well as for their product and power are presented here.

Parallel Combination of Volterra Systems

When a nonlinear operator $\mathcal{H}$ is realized by the parallel combination (or sum) of the Volterra operators $\mathcal{A}$ and $\mathcal{B}$ [Fig. 2(a)], then $\mathcal{H}$ can be represented by a Volterra series whose Volterra operators are obtained by summing at each order the operators representing $\mathcal{A}$ and $\mathcal{B}$ [Fig. 2(b)]

$$\mathcal{H}_j = \mathcal{A}_j + \mathcal{B}_j \quad (j = 0,1,\ldots) \tag{24}$$

The VFRFs of $\mathcal{H}$ can be easily obtained by substituting into Eq. (24) the expressions of $\mathcal{A}$ and $\mathcal{B}$ in the form of Eq. (12), obtaining:

$$\mathcal{H}_j[u] = \int_{\mathbf{\Omega}_j \in \mathbb{R}^j} e^{i\Sigma\mathbf{\Omega}_j t} A_j(\mathbf{\Omega}_j) \prod_{r=1}^{j} dU(\omega_r) + \int_{\mathbf{\Omega}_j \in \mathbb{R}^j} e^{i\Sigma\mathbf{\Omega}_j t} B_j(\mathbf{\Omega}_j) \prod_{s=1}^{j} dU(\omega_s) \tag{25}$$

where A_j and B_j are VFRFs of $\mathcal{A}$ and $\mathcal{B}$, respectively. The comparison of Eqs. (25) and (12) provides

$$H_j(\mathbf{\Omega}_j) = A_j(\mathbf{\Omega}_j) + B_j(\mathbf{\Omega}_j) \quad (j = 0,1,\ldots) \tag{26}$$

Product of Volterra Systems

When an operator $\mathcal{H}$ is realized by the product of the Volterra operators $\mathcal{A}$ and $\mathcal{B}$ [Fig. 3(a)], then its jth-order output $\mathcal{H}_j$ is homogeneous of degree j, which contains all the possible products of the outputs $\mathcal{A}_r$ and $\mathcal{B}_p$ for which $r+p=j$ [Fig. 3(b)]

$$\mathcal{H}_j[u] = \sum_{k=0}^{j} \mathcal{A}_k[u]\mathcal{B}_{j-k}[u] \quad (j = 0,1,\ldots) \tag{27}$$

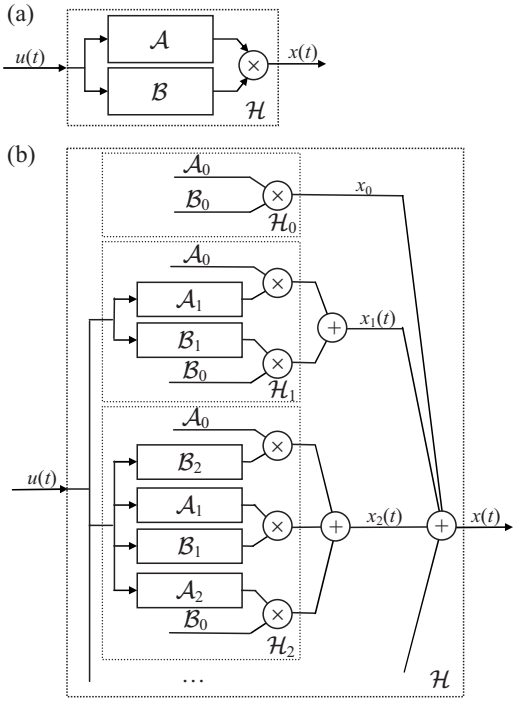

Fig. 3. Block diagram for product of Volterra systems

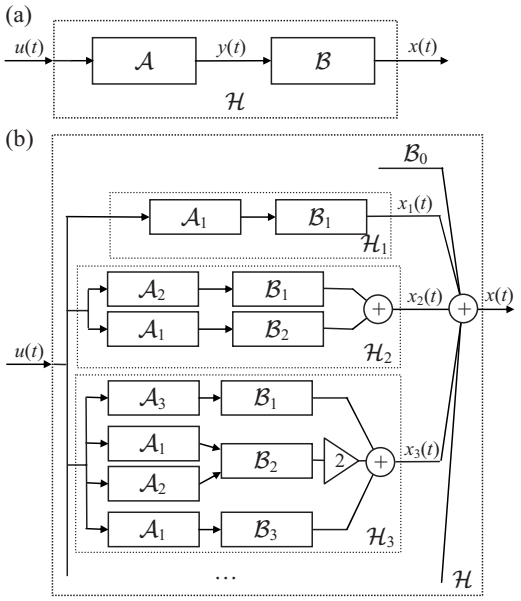

Fig. 4. Block diagram for series combination of Volterra systems

The VFRFs of $\mathcal{H}$ can be obtained by expressing $\mathcal{A}_r$ and $\mathcal{B}_p$ in the form of Eq. (12), resulting in

$$\mathcal{H}_j[u] = \sum_{k=0}^{j} \int_{\mathbf{\Omega}_k \in \mathbb{R}^k} e^{i\Sigma\mathbf{\Omega}_k t} A_k(\mathbf{\Omega}_k) \prod_{r=1}^{k} dU(\omega_r) \times \int_{\mathbf{\Omega}_{j-k} \in \mathbb{R}^{j-k}} e^{i\Sigma\mathbf{\Omega}_{j-k} t} B_{j-k}(\mathbf{\Omega}_{j-k}) \prod_{s=1}^{j-k} dU(\omega_s) \quad (28)$$

To rearrange Eq. (28), let us assume that the vector $\mathbf{\Omega}_j$ is partitioned into the k vectors $\boldsymbol{\theta}_1^{(j,k)}, \ldots, \boldsymbol{\theta}_k^{(j,k)}$ with size, respectively, $\alpha_1^{(j,k)}, \ldots, \alpha_k^{(j,k)}$, such that

$$\alpha_p^{(j,k)} \geq 0 \quad (p = 1, \ldots, k)$$

$$\sum_{p=1}^{k} \alpha_p^{(j,k)} = j \quad (29)$$

Applying this notation, Eq. (28) can be rewritten in the form

$$\mathcal{H}_j[u] = \sum_{\alpha_p^{(j,2)}} \int_{\mathbf{\Omega}_j \in \mathbb{R}^j} e^{i\Sigma\mathbf{\Omega}_j t} A_{\alpha_1^{(j,2)}}(\boldsymbol{\theta}_1^{(j,2)}) B_{\alpha_2^{(j,2)}}(\boldsymbol{\theta}_2^{(j,2)}) \prod_{r=1}^{j} dU(\omega_r) \quad (30)$$

where the summation over $\alpha_p^{(j,k)}$ means that the summation is operated including all the possible sequences $\alpha_1^{(j,k)}, \ldots, \alpha_k^{(j,k)}$ fulfilling Eq. (29). In the specific case of Eq. (30) ($k=2$), the sum is performed for any pair of numbers $\alpha_1^{(j,2)}$ and $\alpha_2^{(j,2)}$ such that $\alpha_1^{(j,2)} + a_2^{(j,2)} = j$. The comparison of Eqs. (30) and (12) provides

$$H_j(\mathbf{\Omega}_j) = \sum_{\alpha_p^{(j,2)}} A_{\alpha_1^{(j,2)}}(\boldsymbol{\theta}_1^{(j,2)}) B_{\alpha_2^{(j,2)}}(\boldsymbol{\theta}_2^{(j,2)}) \quad (31)$$

The expanded version of Eq. (31) is given in the Appendix [Eq. (85)] for $j=0$ to 3.

The results described in Eqs. (27) and (31) can be easily generalized to the case in which a system $\mathcal{H}$ is given by the kth-order power of a system $\mathcal{A}$ (i.e., iterating k times the product of $\mathcal{A}$ by itself). In this case, the jth-order Volterra operator of $\mathcal{H}$ can be written as

$$\mathcal{H}_j[u] = \sum_{\alpha_p^{(j,k)}} \prod_{r=1}^{k} \mathcal{A}_{\alpha_r^{(j,k)}}[u] \quad (32)$$

while its VFRFs result

$$H_j(\mathbf{\Omega}_j) = \sum_{\alpha_p^{(j,k)}} \prod_{r=1}^{k} A_{\alpha_r^{(j,k)}}(\boldsymbol{\theta}_r^{(j,k)}) \quad (33)$$

The summation in Eq. (33) contains several repeated terms due to the presence of all the possible permutations of the sequences $\alpha_p^{(j,k)}$. Retaining in the summation only independent sequences $\alpha_p^{(j,k)}$ (i.e., removing all their redundant permutations), more compact expressions of the VFRFs can be obtained as

$$H_j(\mathbf{\Omega}_j) = \sum_{\substack{\alpha_p^{(j,k)} \\ \text{(no perm.)}}} \frac{k!}{\prod_{s \in \alpha_p^{(j,k)}} N_s(\alpha_p^{(j,k)})!} \prod_{r=1}^{k} A_{\alpha_r^{(j,k)}}(\boldsymbol{\theta}_r^{(j,k)}) \quad (34)$$

where the sum is performed on all the independent sequences $\alpha_p^{(j,k)}$ (i.e., all the permutations are excluded), the product is operated on any distinct number s present in the sequence $\alpha_1^{(j,k)}, \ldots, \alpha_k^{(j,k)}$ and $N_s(\alpha_p^{(j,k)})$ represents the number of times that s appears in the sequence $\alpha_p^{(j,k)}$.

Series Combination of Volterra Systems

When an operator $\mathcal{H}$ comprises the series combination of the two Volterra systems $\mathcal{A}$ and $\mathcal{B}$ [Fig. 4(a)], in such a way that the output of $y=\mathcal{A}[u]$ of the operator $\mathcal{A}$ is the input for the operator $\mathcal{B}$, then its jth-order output can be obtained by summing the output of all the multilinear operator $\mathcal{B}_k\{\cdot, \ldots, \cdot\}$ whose k inputs have an order such that their sum is j. This concept is demonstrated in Fig. 4(b) (for the case in which $\mathcal{A}_0=0$) and can be expressed by the formula

$$\mathcal{H}_j[u] = \sum_{k=1}^{n_{\mathcal{B}}} \sum_{\alpha_p^{(j,k)}} \mathcal{B}_k\{y_{\alpha_1^{(j,k)}}, \ldots, y_{\alpha_k^{(j,k)}}\} \quad (j \geq 1) \tag{35}$$

where $n_{\mathcal{B}}$=order of the Volterra system $\mathcal{B}$ and y_p=pth-order output of $\mathcal{A}$. Introducing the expression of $\mathcal{B}_k$ in the form given by Eq. (12), Eq. (35) can be recast as

$$\mathcal{H}_j[u] = \sum_{k=1}^{n_{\mathcal{B}}} \sum_{\alpha_p^{(j,k)}} \int_{\mathbf{\Omega}_k \in \mathbb{R}^k} e^{i\Sigma\mathbf{\Omega}_k t} B_k(\mathbf{\Omega}_k) \prod_{r=1}^{k} dY_{\alpha_r^{(j,k)}}(\omega_r) \quad (j \geq 1) \tag{36}$$

where dY_p is the frequency-domain counterpart of y_p, and is given by the expression analogous to Eq. (13) in terms of the VFRFs A_k of the operator $\mathcal{A}$. Substituting such expressions into Eq. (36) provides

$$\mathcal{H}_j[u] = \sum_{k=1}^{n_{\mathcal{B}}} \sum_{\alpha_p^{(j,k)}} \int_{\mathbf{\Omega}_k \in \mathbb{R}^k} e^{i\Sigma\mathbf{\Omega}_k t} B_k(\mathbf{\Omega}_k) \times \prod_{r=1}^{k} \left[\int_{\substack{\mathbf{\Omega}'_{\alpha_r^{(j,k)}} \in \mathbb{R}^{\alpha_r^{(j,k)}} \\ \Sigma\mathbf{\Omega}'_{\alpha_r^{(j,k)}} = \omega_r}} A_{\alpha_r^{(j,k)}}(\mathbf{\Omega}'_{\alpha_r^{(j,k)}}) \prod_{s=1}^{\alpha_r^{(j,k)}} dU(\omega'_s) \right] \tag{37}$$

where each of the integrals inside the parenthesis is performed with respect to the integration variable $\mathbf{\Omega}_{\alpha_r^{(j,k)}} = [\omega_1, \ldots, \omega_{\alpha_r^{(j,k)}}]^T$ ($r=1, \ldots, k$), on a subspace of $\mathbb{R}^j$ with dimension $\alpha_r^{(j,k)} - 1$; collecting these integrals, Eq. (37) results

$$\mathcal{H}_j[u] = \sum_{k=1}^{n_{\mathcal{B}}} \sum_{\alpha_p^{(j,k)}} \int_{\mathbf{\Omega}_k \in \mathbb{R}^k} e^{i\Sigma\mathbf{\Omega}_k t} B_k(\mathbf{\Omega}_k) \times \int_{\substack{\mathbf{\Omega}'_j \in \mathbb{R}^j \\ \bigcup_{q=1}^{k} \Sigma\boldsymbol{\theta}'_{\alpha_q^{(j,k)}} = \omega_q}} \prod_{r=1}^{k} A_{\alpha_r^{(j,k)}}(\boldsymbol{\theta}'^{(j,k)}_r) \prod_{s=1}^{j} dU(\omega'_s) \tag{38}$$

in which the vectors $\boldsymbol{\theta}'^{(j,k)}_r$ represent the partition of $\mathbf{\Omega}'_j$. The two integrals in Eq. (38) are computed on two orthogonal subspaces of $\mathbb{R}^j$ with dimensions k and $j-k$, respectively, and can be formally joined together noting that, when the constraint prescribed on the domain of the second integral is fulfilled, it results in $\Sigma\mathbf{\Omega}_k = \Sigma\mathbf{\Omega}_j$

$$\mathcal{H}_j[u] = \sum_{k=1}^{n_{\mathcal{B}}} \sum_{\alpha_p^{(j,k)}} \int_{\mathbf{\Omega}_j \in \mathbb{R}^j} e^{i\Sigma\mathbf{\Omega}_j t} B_k(\mathbf{S}^{(j,k)}\mathbf{\Omega}_j) \times \prod_{r=1}^{k} A_{\alpha_r^{(j,k)}}(\boldsymbol{\theta}_r^{(j,k)}) \prod_{s=1}^{j} dU(\omega_s) \tag{39}$$

where $\mathbf{S}^{(j,k)}$ is a matrix of dimension $k \times j$ defined as

$$\mathbf{S}^{(j,k)} = \begin{bmatrix} \overbrace{1 \cdots 1}^{\alpha_1^{(j,k)}} & & & 0 \\ & \overbrace{1 \cdots 1}^{\alpha_2^{(j,k)}} & & \\ & & \cdots & \\ 0 & & & \overbrace{1 \cdots 1}^{\alpha_k^{(j,k)}} \end{bmatrix} \tag{40}$$

A comparison of Eqs. (39) and (12) provides

$$H_j(\mathbf{\Omega}_j) = \sum_{k=1}^{n_{\mathcal{B}}} \sum_{\alpha_p^{(j,k)}} B_k(\mathbf{S}^{(j,k)}\mathbf{\Omega}_j) \prod_{r=1}^{k} A_{\alpha_r^{(j,k)}}(\boldsymbol{\theta}_r^{(j,k)}) \quad (j \geq 1) \tag{41}$$

in which duplicated sequences can be eliminated, as it has been shown for Eqs. (33) and (34). Eq. (41) {expanded in the Appendix [Eq. (86)] for $n_{\mathcal{B}}=3$ and $j=1$ to 3} has been illustrated for $j \geq 1$, however its validity can also be extended to $j=0$ by just adding the term B_0 to account for a possible zeroth-order output of $\mathcal{B}$. In this case, however, a much simpler expression can be derived

$$H_0 = \sum_{k=0}^{n_{\mathcal{B}}} B_k(0) A_0^k \tag{42}$$

It is worth noting that the jth-order term of Eq. (41) contains all the VFRFs A_k for $k \leq j$ and that, if $A_0=0$, then all the sequences containing an $\alpha_r^{(j,k)}=0$ do not give any contribution to the sum. A consequence of these features is that H_j contains only the VFRFs, B_k, with $k \leq j$ and A_j appears only once, multiplied by B_1. In this case, Eq. (41) can be rewritten in the simplified form

$$H_j(\mathbf{\Omega}_j) = B_1(\Sigma\mathbf{\Omega}_j) A_j(\mathbf{\Omega}_j) + \sum_{k=2}^{j} \sum_{\alpha_p^{(j,k)}} B_k(\mathbf{S}^{(j,k)}\mathbf{\Omega}_j) \times \prod_{r=1}^{k} A_{\alpha_r^{(j,k)}}(\boldsymbol{\theta}_{\alpha_r^{(j,k)}}) \quad (j \geq 1) \tag{43}$$

where the only term in A_j has been extracted from the summation. Besides, if $\mathcal{B}$ is a linear homogeneous operator (i.e., contains only the first-order term $\mathcal{B}_1$), then Eq. (41) becomes very simple, resulting

$$H_j(\mathbf{\Omega}_j) = B_1(\Sigma\mathbf{\Omega}_j) A_j(\mathbf{\Omega}_j) \tag{44}$$

while if, on the contrary, $\mathcal{A}$ is a linear homogeneous operator, then Eq. (41) becomes

$$H_j(\mathbf{\Omega}_j) = B_j(\mathbf{\Omega}_j) \prod_{r=1}^{j} A_1(\omega_r) \tag{45}$$

VFRFs for a Class of Dynamical Systems

A fairly general dynamical system can be represented by the following equation:

$$\mathcal{D}[x] = \mathcal{F}[x, u] \tag{46}$$

where u=input and x=output, while $\mathcal{D}$ and $\mathcal{F}$ are two nonlinear (in general) operators. Let us assume that the input and output can be related by an operator $\mathcal{H}$ through Eq. (1), then, Eq. (46) can be rewritten, eliminating the output, as

$$\mathcal{L}[u] = \mathcal{D}(\mathcal{H}[u]) = \mathcal{F}(\mathcal{H}[u], u) = \mathcal{R}[u] \tag{47}$$

in which the left-hand-side operator $\mathcal{L}$ and the right-hand-side operator $\mathcal{R}$ can be reviewed as assemblages of operators including the unknown operator $\mathcal{H}$ and their VFRFs, L_j and R_j, can be constructed, at least formally, by the assemblage rules described above, resulting in functions of the VFRFs H_j of $\mathcal{H}$. The VFRFs H_j are obviously unknown, but can be evaluated equating L_j and R_j at each order leading to a set of algebraic equations:

$$L_j(\mathbf{\Omega}_j) = R_j(\mathbf{\Omega}_j) \quad (j = 0, \ldots, n) \tag{48}$$

According to the assemblage rules reported above, L_j and R_j depend only on H_k with $k \leq j$; besides, with the only exception of $j=0$, they are linear in H_j. This means that if the VFRFs of $\mathcal{H}$ are known up to the order $j-1$, then H_j can be obtained by solving an algebraic linear equation. Eq. (48) can therefore be solved in a cascading manner beginning with the static solution (zeroth order) and subsequently solving single linear equations.

Formal simplifications can be obtained if Eq. (46) is written in such a way to have the operator $\mathcal{D}$ linear (keeping all the nonlinearities on the right hand side) and assuming that the dynamical system $\mathcal{H}$ does not have a zeroth-order output ($x_0=0$). These results can often be achieved quite easily by manipulating Eq. (46) in a suitable way. If $\mathcal{D}$ is linear, indeed, it can be easily inverted [the FRF of $\mathcal{D}^{-1}$ is $D(\omega)^{-1}$, $D(\omega)$ being the FRF of $\mathcal{D}$] and brought on the right-hand side of Eq. (47). The left-hand side of Eq. (48), therefore, results directly in H_j since $x_0=0$. Whereas, the jth-order VFRF of the right-hand side can be expressed through a relationship analogous to Eq. (43) in which the term containing H_j is isolated and can be brought on the left-hand side of the equation. The examples presented in the Applications and Numerical Examples Section further illustrate this concept.

Response of a Volterra System to Gaussian Input

The evaluation of the response of a Volterra system to a Gaussian stationary input was treated by Bedrosian and Rice (1971), developing formal expressions for the first few statistical moments of the response, for its autocorrelation function, as well as for its PSD. In this section, these results are reproduced through the concept of a composite system, obtaining fairly general results expressed by formally simple relationships.

As a first step, necessary to obtain the above mentioned result, let us evaluate the expected value of the output of an nth-order Volterra system $\mathcal{H}$

$$E(\mathcal{H}[u]) = \sum_{j=0}^{n} E(\mathcal{H}_j[u]) = \sum_{j=0}^{n} \int_{\mathbf{\Omega}_j \in \mathbb{R}^j} e^{i\Sigma\mathbf{\Omega}_j t} H_j(\mathbf{\Omega}_j) E\left[\prod_{r=1}^{j} dU(\omega_r)\right] \tag{49}$$

If the input $u(t)$ is Gaussian and zero mean, then the expectation in Eq. (49) can be expressed through Eq. (9), leading to the expression:

$$E(\mathcal{H}[u]) = \sum_{\substack{j=0 \\ j \text{ even}}}^{n} \frac{j!}{(j/2)!2^{j/2}} \int_{\substack{\mathbf{\Omega}_j \in \mathbb{R}^j \\ \mathbf{D}_j\mathbf{\Omega}_j=\mathbf{0}}} H_j(\mathbf{\Omega}_j) \prod_{r=1}^{j/2} S_{uu}(\omega_r) d\mathbf{\Omega}_j \tag{50}$$

where the summation is restricted to the even terms and $\mathbf{D}_j = [\mathbf{I}_{j/2}\mathbf{I}_{j/2}]$, $\mathbf{I}_{j/2}$ being the identity matrix of size $j/2$. The expected value of the output of an nth-order Volterra system is obtained, according to Eq. (50), by integrating the VFRFs with even order, over domains with dimension up to $n/2$. The expanded version of Eq. (50) is given in the Appendix for $n=4$ [Eq. (87)].

The kth-order statistical moment of the output of an nth-order Volterra system $\mathcal{H}$ can be calculated evaluating the VFRFs of the k-power system $\mathcal{H}^k$ through Eq. (34) and calculating the expectation by Eq. (50). It results

$$m_k(\mathcal{H}[u]) = \sum_{\substack{j=0 \\ j \text{ even}}}^{nk} \frac{j!}{(j/2)!2^{j/2}} \times \sum_{\alpha_p^{(j,k)}} \int_{\substack{\mathbf{\Omega}_j \in \mathbb{R}^j \\ \mathbf{D}_j\mathbf{\Omega}_j=\mathbf{0}}} \text{sym}\left[\prod_{r=1}^{k} H_{\alpha_r^{(j,k)}}(\boldsymbol{\theta}_r^{(j,k)})\right] \prod_{s=1}^{j/2} S_{uu}(\omega_s) d\mathbf{\Omega}_j \tag{51}$$

where integrals have dimension up to $nk/2$ and contain the symmetrical VFRFs of $\mathcal{H}$, as well as the PSD of the input. Explicit expressions of the first four statistical moments ($j=1$ to 4) for a third-order Volterra system ($n=3$) are given in (Li et al. 1995). As an example, Eq. (51) is expanded in the Appendix [Eq. (88)] for $k=2$ and $n=3$.

An expression for the autocorrelation function $R_{xx}(T)$ of the output $x(t)$ can be evaluated following an analogous procedure, evaluating the expectation [through Eq. (50)] of a system realized by the product of $\mathcal{H}[u(t)]$ and $\mathcal{H}[u(t+T)]$ whose VFRFs are obtained applying Eqs. (17) and (31)

$$R_{xx}(T) = \sum_{\substack{j=0 \\ j \text{ even}}}^{nk} \frac{j!}{(j/2)!2^{j/2}} \times \sum_{\alpha_p^{(j,2)}} \int_{\substack{\mathbf{\Omega}_j \in \mathbb{R}^j \\ \mathbf{D}_j\mathbf{\Omega}_j=\mathbf{0}}} \text{sym}[H_{\alpha_1^{(j,2)}}(\boldsymbol{\theta}_1^{(j,2)}) \times H_{\alpha_2^{(j,2)}}(\boldsymbol{\theta}_2^{(j,2)}) e^{-i\Sigma\boldsymbol{\theta}_2^{(j,2)}T}] \prod_{s=1}^{j/2} S_{uu}(\omega_s) d\mathbf{\Omega}_j \tag{52}$$

The PSD of the output can be obtained by a Fourier transform of Eq. (52), however no compact general expression is available due to the necessity of symmetrizing the VFRFs before performing the integration. An explicit expression for the PSD output of a third-order Volterra series is reported in the Appendix [Eq. (89)].

The computation of the integrals reported in Eqs. (51) and (52) can be computationally intensive when high-order statistics of a high-order Volterra series are required. In these cases, rather than using classical quadrature schemes, a MCS based scheme may be more effective.

Applications and Numerical Examples

In order to demonstrate the application of the described technique, the VFRFs of some mechanical systems of relevant interest in wind and offshore engineering will be determined. The examples are introduced with increasing level of complexity in obtaining the VFRFs using the assemblage rules described in the Evaluation of VFRFs Section. The response to a stationary random input is computed by the formulation discussed in the Response of a Volterra System to Gaussian Input Section considering different levels of approximation corresponding to Volterra models with order $n=1$ to 5. These results are compared to the results obtained by the time-domain integration of the equation of motion within an MCS framework. The PDF of the re-

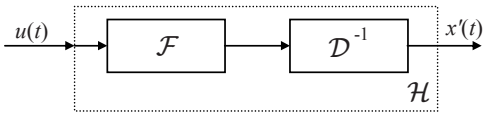

Fig. 5. Example 1: block diagram for Eq. (55)

sponse is estimated by using a third-order polynomial translation model based on the first four cumulants (Grigoriu 1984; Winterstein 1985; Tognarelli et al. 1997b).

Example 1: Polynomial Input

The first example is constituted by a wind-excited single-degree-of-freedom (DOF) point-like structure whose equation of motion is expressed in the form

$$m\ddot{x} + c\dot{x} + kx = k_d(U+u)^2 \tag{53}$$

where x (the output)=structural displacement and u (the input)=wind turbulence modeled as a zero mean, stationary, Gaussian random process; U=mean wind velocity and m, c, and k=the mass, damping coefficient, and stiffness, respectively; k_d=coefficient depending on the geometric and aerodynamic properties of the structure. It is worth noting that the aerodynamic force introduced in Eq. (53) is necessarily positive (due to the square), while according to the quasi-steady assumption, the drag force should have the same sign of the wind velocity $U+u$, which since u has Gaussian distribution, can be negative. This discrepancy, however, has no consequences since the mean velocity U is typically much larger than the turbulent fluctuation u, making the probability of having a negative value for $U+u$ extremely low.

The zeroth-order response of the system can be readily calculated from Eq. (53), letting $u=0$ and eliminating all the time derivatives of x, resulting in

$$x_0 = \frac{k_d}{k}U^2 \tag{54}$$

while, the fluctuating part of the response $x'=x-x_0$ is given by the composite system (Fig. 5)

$$x' = \mathcal{H}[u] = \mathcal{D}^{-1}(\mathcal{F}[u]) \tag{55}$$

in which $\mathcal{D}$ represents the left-hand side operator of Eq. (53), while $\mathcal{F}[u]=2k_dUu+k_du^2$.

The only nonlinearity in Eq. (55) is on the input side and has polynomial form. The VFRFs of the operators $\mathcal{D}$ and $\mathcal{F}$ can be obtained applying the rules described in the Evaluation of the VFRFs Section, resulting

$$D_1(\omega) = -\omega^2 m + i\omega c + k \tag{56}$$

$$F_1 = 2k_dU; \quad F_2 = k_d \tag{57}$$

The VFRFs of the composite system can be obtained by applying the rule given by Eq. (44), resulting $H_j=0$ for $j\neq 1, 2$ and

$$H_1(\omega) = 2k_dUD_1^{-1}(\omega)$$

$$H_2(\omega_1,\omega_2) = k_dD_1^{-1}(\omega_1+\omega_2) \tag{58}$$

The wind turbulence u is defined by the PSD (Solari and Piccardo 2001)

Table 1. Example 1: Statistics of the Response

	Mean (m)	SD (m)	Skewness	COE
MCS	1.90×10^{-1}	1.43×10^{-1}	8.77×10^{-1}	1.14
Second-order Volterra model	1.89×10^{-1}	1.44×10^{-1}	8.77×10^{-1}	1.15
Linear	1.71×10^{-1}	1.39×10^{-1}	—	—

$$S_{uu}(\omega) = \sigma_u^2 \frac{0.546\dfrac{L_u}{U}}{\left(1+1.640|\omega|\dfrac{L_u}{U}\right)^{5/3}} \tag{59}$$

where σ_u=5 m/s, and L_u=120 m are, respectively, the root-mean-square and the integral length scale of turbulence; the mean wind velocity is assumed as U=15 m/s. The mechanical system is defined by the parameters m=100 kg, $\omega_0=\sqrt{k/m}$=6.28 rad/s, $\xi=c/2m\omega_0$=0.05, and k_d=3.0 kg/m.

The response statistics up to the fourth order [mean μ, standard deviation (SD) σ, skewness γ_3, coefficient of excess (COE) γ_4] are obtained by evaluating the integrals involving VFRFs according to Eq. (51) and reported in Table 1. The second-order Volterra model defined by Eqs. (58) rigorously represents the dynamical system given by Eq. (55), hence the statistics of its response should be considered as exact within the approximation of the integration scheme. The response of the linear model obtained letting $H_2=0$ is also shown in Table 1. In the present case, the integration was performed by a fourth-order quadrature scheme with the frequency interval between 10^{-3} and 10 rad/s, discretized at 500 points, and distributed according to an exponential law (Carassale and Solari 2006). The results obtained in this manner for the second-order Volterra system are very close to the values obtained by the time-domain MCS with a total simulation length about 1.3×10^6 s. The linear approximation results in a slight underestimation of the mean value (10%) and of the SD (3%) of the response; obviously, no information can be obtained concerning the skewness and COE.

Fig. 6 compares the PSD of the response calculated by the time-domain MCS and by the first- and second-order Volterra

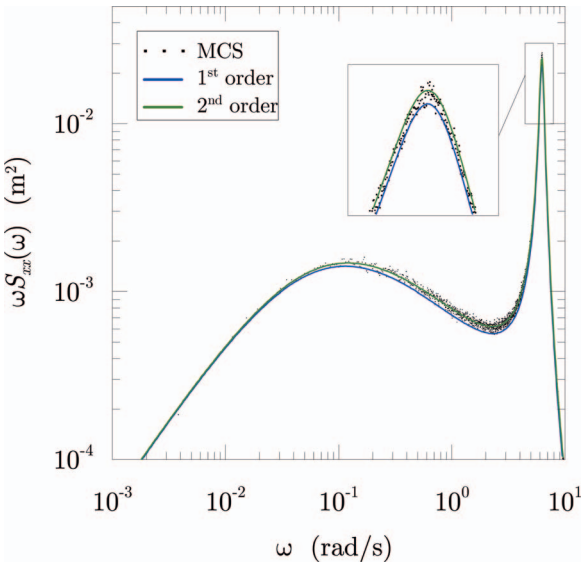

Fig. 6. (Color) Example 1: PSD of the response by time-domain MCS and by first- and second-order Volterra models.

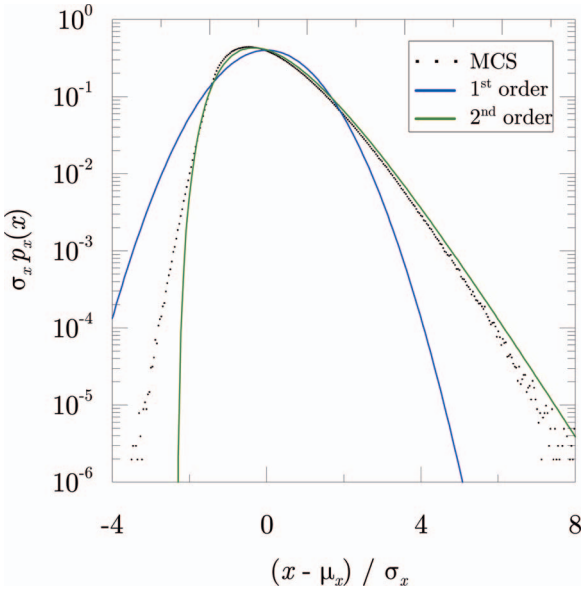

Fig. 7. (Color) Example 1: PDF of the response by the time-domain MCS and Volterra models with order $n=1$ and 2, nondimensionalized by the SD, and centered at the mean value obtained by MCS

models. The second-order Volterra model and MCS provide practically identical results, while the linear model slightly underestimates the target spectrum.

Fig. 7 compares the PDF of the response estimated by time-domain MCS and by first- and second-order Volterra models. The plots are nondimensionalized by the SD centered at the mean value obtained by the MCS. The Gaussian PDF provided by the first-order model departs from the results of the simulation, while the PDF obtained by the second-order model is quite accurate on the right tail and slightly underestimates on the left tail. It must be emphasized that in this case, the second-order Volterra model is exact and the observed discrepancy is due to the selected PDF model.

Example 2: Polynomial Input with Response Feedback

For relatively flexible structures, the wind force needs to be evaluated in terms of relative wind-structure velocity and Eq. (53) must be accordingly recasted

$$m\ddot{x} + c\dot{x} + kx = k_d(U + u - \dot{x})^2 \tag{60}$$

The zeroth-order output x_0 is still given by Eq. (54), while the operator $\mathcal{H}$ providing the time-varying response $x' = x - x_0$ is described by the block diagram given in Fig. 8 and represented by the relationship

$$x' = \mathcal{H}[u] = \mathcal{D}^{-1}(\mathcal{F}[u - \dot{x}]) = \mathcal{D}^{-1}\left[\mathcal{F}\left(u - \frac{d}{dt}\mathcal{H}[u]\right)\right] \tag{61}$$

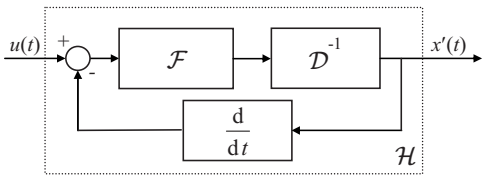

Fig. 8. Example 2: block diagram for Eq. (61)

in which the operators $\mathcal{D}$ and $\mathcal{F}$ are defined through the VFRFs given by Eqs. (56) and (57), respectively.

In order to evaluate the VFRFs of the right-hand side of Eq. (61), let us consider the two operators

$$\mathcal{A}[u] = u - \frac{d}{dt}\mathcal{H}[u]$$

$$\mathcal{B}[u] = \mathcal{F}(\mathcal{A}[u]) \tag{62}$$

The output of the operator $\mathcal{A}$ represents the wind-structure relative velocity and its VFRFs can be easily obtained as functions of the VFRFs of $\mathcal{H}$ (which are unknown), by applying Eqs. (15), (26), and (44), resulting $A_0=0$

$$A_1(\omega) = 1 - i\omega H_1(\omega)$$

$$A_j(\boldsymbol{\Omega}_j) = -i\Sigma\boldsymbol{\Omega}_j H_j(\boldsymbol{\Omega}_j) \quad j \geq 2 \tag{63}$$

The operator $\mathcal{B}$, whose output represents the aerodynamic force, is characterized by the VFRFs obtained according to Eq. (41) as $B_0=0$,

$$B_1(\omega) = 2k_d U A_1(\omega)$$

$$B_j(\boldsymbol{\Omega}_j) = 2k_d U A_1(\Sigma\boldsymbol{\Omega}_j) + k_d \sum_{\alpha_p^{(j,2)}} \prod_{r=1}^{2} A_{\alpha_r^{(j,2)}}(\boldsymbol{\theta}_{\alpha_r^{(j,2)}}) \quad j \geq 2 \tag{64}$$

Finally, composing $\mathcal{B}$ in series with $\mathcal{D}^{-1}$ through Eq. (44) {or alternatively equating the VFRFs of $\mathcal{B}$ and $\mathcal{D}(\mathcal{H}[u])$}, provides $H_0=0$

$$H_1(\omega) = 2k_d U \hat{D}(\omega)^{-1}$$

$$H_j(\boldsymbol{\Omega}_j) = k_d \hat{D}(\Sigma\boldsymbol{\Omega}_j)^{-1} \sum_{\alpha_p^{(j,2)}} \prod_{r=1}^{2} A_{\alpha_r^{(j,2)}}(\boldsymbol{\theta}_{\alpha_r^{(j,2)}}) \quad j \geq 2 \tag{65}$$

where $\hat{D}(\omega) = D(\omega) + 2k_d U i\omega$. The VFRFs H_j are given as functions of the VFRFs A_j, which in turn depend on H_j. However, it is worth noting that, since $A_0=0$, H_j depends only on A_k for $k<j$, thus each VFRF H_j can be directly obtained by Eqs. (65), evaluating the expressions at each order in a cascade manner. The integration of the VFRFs was performed by an MCS-based quadrature scheme, while the time-domain MCS involved a total simulation length of about 1.3×10^6 s.

Fig. 9 shows the mean (a), SD (b), skewness (c), and COE (d) of the response x evaluated by Eq. (51), retaining one to five terms in the Volterra model defined through the VFRFs given by Eqs. (63) and (65). Unlike in the previous example, the first two terms of the Volterra series do not rigorously represent the given dynamical system; however, the role of the higher-order terms in the evaluation of the statistics up to the fourth order is rather marginal as noted from the comparison with the values obtained by the time-domain MCS (dashed line).

Fig. 10 shows the PSD of the response evaluated by time-domain MCS and by first- and second-order Volterra models. Spectra obtained by higher-order models have not been reported since they coincide with second-order result. Similar to Example 1, the linear model slightly underestimates the target spectrum.

Fig. 11 compares the PDF obtained by time-domain MCS and by Volterra models with order $n=1$ to 4 (the fifth-order term of the series does not provide any notable contribution to the PDF).

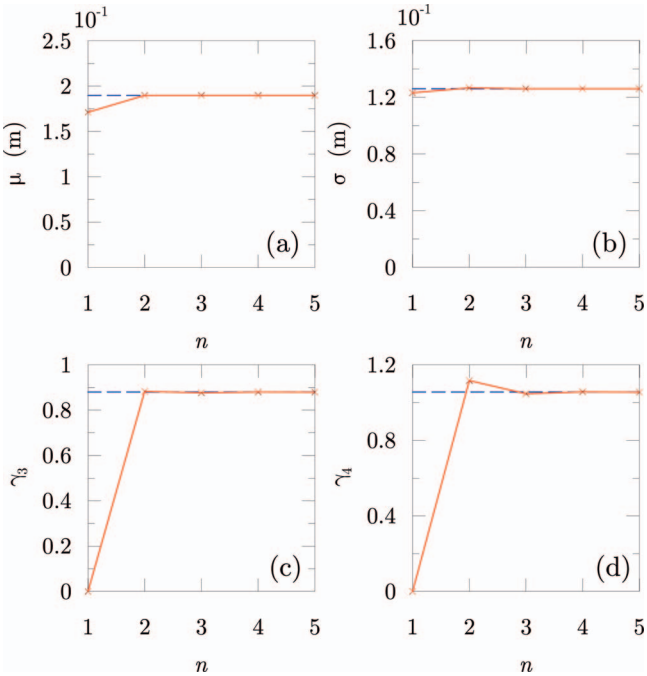

Fig. 9. (Color) Example 2: mean (a); SD (b); skewness (c); and COE (d) of the response by nth-order Volterra series (×) and time-domain MCS (dashed line)

The plots are nondimensionalized by the SD and centered at the mean value obtained by the MCS. Like in Example 1, the Gaussian PDF provided by the linear model departs significantly from the target distribution, while the second-order model gives accurate results.

Example 3: Nonpolynomial Input

Let us consider a linear single-DOF point-like structure excited by the ocean-wave force modeled according to the Morison equation [e.g., Chakrabarti (1990)]. Its equation of motion is given by

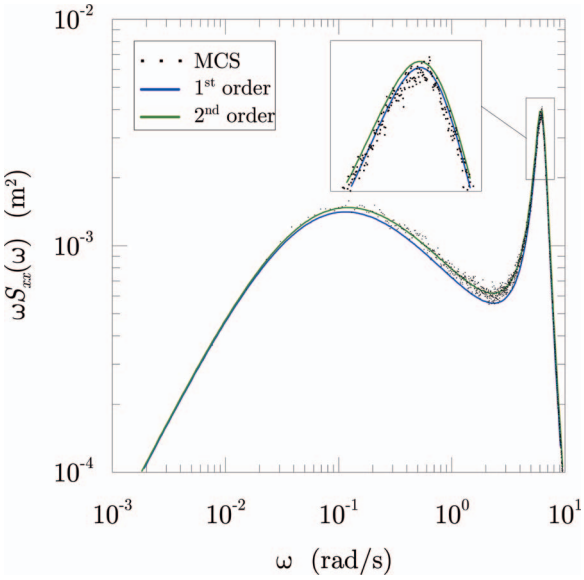

Fig. 10. (Color) Example 2: PSD of the response by time-domain MCS and by first- and second-order Volterra models

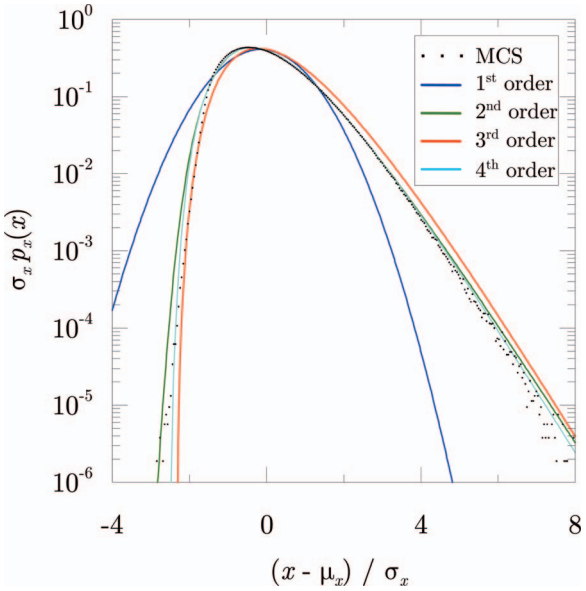

Fig. 11. (Color) Example 2: PDF of the response by the time-domain MCS and Volterra models with order $n=1$ to 4, nondimensionalized by the SD, and centered at the mean value obtained by MCS

$$m\ddot{x} + c\dot{x} + kx = k_d(U+u)|U+u| + k_m\dot{u} \tag{66}$$

where the input u represents the water-particle velocity modeled, based on the linear wave theory as a zero-mean Gaussian random process; U=current velocity; and k_d and k_m=coefficients depending on the geometric and hydrodynamic properties of the structure. The first term of the force, referred to as the viscous component, is a nonlinear function of the driving process $u(t)$, while the second term, referred to as the inertial component, is in terms of a linear transformation of the input. The viscous term contains a memoryless nonlinearity that, in order to obtain a Volterra-series representation, must be approximated by a polynomial

$$g(u) = (U+u)|U+u| \simeq \sum_{r=0}^{n} a_r u^r \tag{67}$$

where a_r $(r=0,\ldots,n)$=coefficients to be estimated according to the rules described in the Polynomial and Memoryless Nonlinearities Section. The zeroth-order output of the system can be readily obtained letting $u=0$ in Eq. (66) and removing the time derivatives, resulting

$$x_0 = \frac{k_d a_0}{k} \tag{68}$$

while the fluctuating output $x' = x - x_0$ is given by the composite system (Fig. 12)

$$x' = \mathcal{H}[u] = \mathcal{D}^{-1}(\mathcal{G}[u] + \mathcal{F}[u]) \tag{69}$$

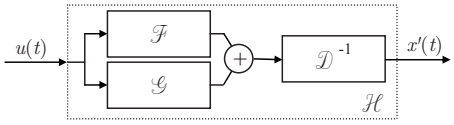

Fig. 12. Example 3: block diagram for Eq. (69)

Table 2. Coefficients for Polynomial Approximation Employed in Examples 3 and 5

Approximation order	Polynomial coefficients					
	a_0	a_1	a_2	a_3	a_4	a_5
1	2.90	3.20	—	—	—	—
2	1.60	3.20	4.38×10^{-1}	—	—	—
3	1.60	2.04	4.38×10^{-1}	1.30×10^{-1}	—	—
4	1.31	2.04	6.34×10^{-1}	1.30×10^{-1}	-1.10×10^{-2}	—
5	1.31	1.84	6.34×10^{-1}	1.74×10^{-1}	-1.10×10^{-2}	-1.46×10^{-3}

in which $\mathcal{D}$ represents the left-hand side of Eq. (66), while $\mathcal{F}$ and $\mathcal{G}$ represent the elementary systems:

$$\mathcal{F}[u] = k_m \frac{du}{dt}; \quad \mathcal{G}[u] = k_d \sum_{r=1}^{n} a_r u^r \tag{70}$$

whose VFRFs result in $F_j=0$ for $j\neq 1$, $G_j=0$ for $j=0$ and $j>n$,

$$F_1(\omega) = i\omega k_m$$

$$G_j(\mathbf{\Omega}_j) = k_d a_j \quad (j=1,\ldots,n) \tag{71}$$

Applying the assemblage rules given in Eqs. (26) and (44), the VFRFs of the operator $\mathcal{H}$ result in $H_0=0$,

$$H_1(\omega) = D(\omega)^{-1}(a_1 + i\omega k_m)$$

$$H_j(\mathbf{\Omega}_j) = D(\Sigma\mathbf{\Omega}_j)^{-1} k_d a_j \quad (j=2,\ldots,n) \tag{72}$$

The water-particle velocity u at the mean water level (MWL) is assumed to be provided by a linear transformation of the wave surface elevation η, and its PSD is given by

$$S_{uu}(\omega) = \omega^2 S_{\eta\eta}(\omega) \tag{73}$$

where $S_{\eta\eta}(\omega)$=PSD of the wave elevation which in the present numerical application is modeled by the JONSWAP spectrum [e.g., Chakrabarti (1990)]

$$S_{\eta\eta}(\omega) = \frac{15H_s^2}{16(\gamma+5)} \frac{\omega_p^4}{|\omega^5|} \exp\left(-\frac{5\omega_p^4}{4\omega^4}\right) \gamma^{\exp[-(\omega-\omega_p)^2/2\xi^2\omega_p^2]} \tag{74}$$

where $\omega_p=2\pi/T_p$, $T_p=20$ s is the peak wave period; $H_s=16$ m is the significant wave height; and $\gamma=1$ is the peakedness factor. The current velocity is $U=1$ m/s. The structural parameters used in Eq. (66) are $m=8.8\times10^6$ kg, $k=3.57\times10^7$ N/m (corresponding to the natural circular frequency $\omega_0=3.14$ rad/s), and $\xi=c/(2m\omega_0)=0.04$. The hydrodynamic parameters are $k_d=3\times10^5$ kg/m and $k_m=3\times10^3$ kg.

The integration of the VFRFs was performed by an MCS-based quadrature scheme while the time-domain MCS involved a total simulation length of about 6.5×10^6 s. Table 2 shows the polynomial coefficients $a_r(r=1,\ldots,n)$ adopted for the approximation of the viscous term of the Morison equation [Eq. (67)], obtained by Eq. (21) for the order of approximation $n=1$ to 5.

Fig. 13 shows the mean (a), SD (b), skewness (c), and COE (d) of the response x, obtained by the Volterra models with orders $n=1$ to 5 through the integration of their VFRFs defined by Eqs. (72). The results of the time-domain MCS are represented by dashed lines. It appears that the mean value of the response is correctly approximated by retaining two terms in the Volterra series, while three, four, and five terms are needed to obtain an accurate estimation of SD, skewness, and COE, respectively.

Fig. 14 shows the PSD of the response evaluated by the time-domain MCS and by Volterra models with order $n=1$ to 4 (the fifth-order term has been omitted since it does not provide any visible contribution to the PSD). The third-order Volterra system provides results very close to the MCS. The first- and second-order models tend to underestimate the PSD in the frequency ranges far from the wave peak frequency; in particular, the first-order model, being unable to detect sub- and superharmonics of the response, strongly underestimates the PSD in the low-frequency range where the wave excitation practically vanishes. The contribution of the fourth-order term is very limited and is visible only at the resonance frequency (frame in Fig. 14).

Fig.15 compares the PDF of the response obtained by time-domain MCS and Volterra models with order $n=1$ to 5. The plots are nondimensionalized by the SD and centered at the mean value obtained by MCS. The third-order model provides a good approximation of the target PDF; however, the effect of the fourth and fifth-order terms is clearly visible.

Example 4: Nonpolynomial Input with Response Feedback

When offshore structures are very flexible, as in the case of floaters, the Morison-type force introduced in Eq. (66) should be modified to take into account the effect of the structural velocity

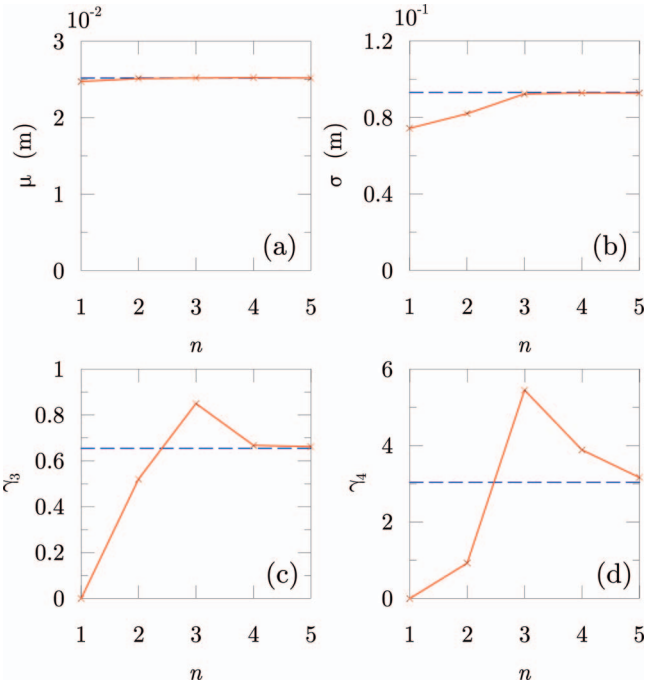

Fig. 13. (Color) Example 3: mean (a); SD (b); skewness (c); and COE (d) of the response by nth-order Volterra series (×) and time-domain MCS (dashed line)

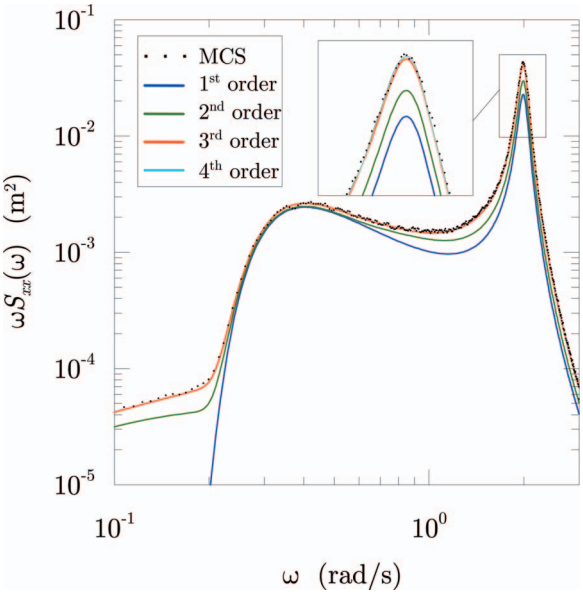

Fig. 14. (Color) Example 3: PSD of the response by time-domain MCS and Volterra models with order $n=1$ to 4

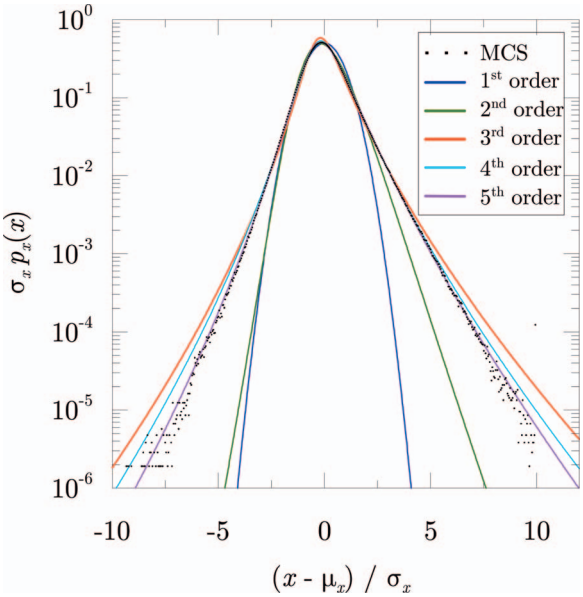

Fig. 15. (Color) Example 3: PDF of the response by the time-domain MCS and Volterra models with order $n=1$ to 5, nondimensionalized by the SD, and centered at the mean value obtained by MCS

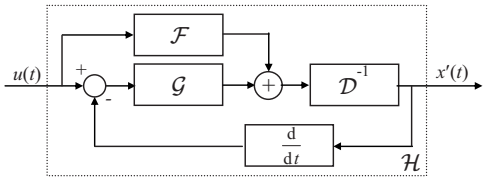

Fig. 16. Example 4: block diagram for Eq. (76)

$$m\ddot{x} + c\dot{x} + kx = k_d(U + u - \dot{x})|U + u - \dot{x}| + k_m\dot{u} \tag{75}$$

The presence of the structural velocity in the viscous term introduces a further nonlinearity (feedback-type) and the dynamical system can be represented as in Fig. 16. The expression of the zeroth-order response [Eq. (68)] is not modified by the introduction of this new nonlinearity since the feedback operator has no zeroth-order term; while the operator $\mathcal{H}$ is now represented as:

$$x' = \mathcal{H}[u] = \mathcal{D}^{-1}\left\{\mathcal{G}\left(u - \frac{d}{dt}\mathcal{H}[u]\right) + \mathcal{F}[u]\right\} \tag{76}$$

The operators $\mathcal{F}$ and $\mathcal{G}$ are formally the same as for Example 3, but the coefficients a_r used for the polynomial approximation of the viscous component of the hydrodynamic force must be calibrated on the basis of the statistical properties of the relative velocity $u-\dot{x}$ which is unknown. This requires some iteration in the solution procedure. Besides, since the relative velocity is non-Gaussian, the estimation of the polynomial coefficients becomes significantly more complicated, as discussed in Tognarelli and Kareem (2001). The polynomial coefficients adopted in the numerical analysis are given in Table 3.

The VFRFs of the operator $\mathcal{H}$ can be obtained applying the corresponding assemblage rules. Like Example 2, the VFRFs are given below

$$H_0 = 0$$

$$H_1(\omega) = \hat{D}(\omega)^{-1}(a_1 + i\omega k_m)$$

$$H_j(\boldsymbol{\Omega}_j) = \hat{D}(\boldsymbol{\Omega}_j)^{-1}\sum_{k=2}^{j} a_k \sum_{\alpha_p^{(j,k)}} \prod_{r=1}^{k} A_{\alpha_r^{(j,k)}}(\boldsymbol{\theta}_{\alpha_r^{(j,k)}}) \quad j \geq 2 \tag{77}$$

where A_j are defined in Eq. (63), while $\hat{D}$ is given by

$$\hat{D}(\omega) = D(\omega) + i\omega a_1 \tag{78}$$

$D(\omega)$ being defined by Eq. (56).

The numerical results are obtained considering the sea state defined for the previous example and the structural parameters: $m=7.13\times10^7$ kg, $k=2.81\times10^5$ N/m ($\omega_0=6.28\times10^{-2}$ rad/s), and $\xi=0.05$. The hydrodynamic parameters are $k_d=6\times10^5$ kg/m and $k_m=4\times10^7$ kg. The integration of Eq. (51) for

Table 3. Coefficients for Polynomial Approximation Employed in Example 4

	Polynomial coefficients					
Approximation order	a_0	a_1	a_2	a_3	a_4	a_5
1	1.57	2.15	—	—	—	—
2	1.08	2.15	8.96×10^{-1}	—	—	—
3	1.08	1.87	7.96×10^{-1}	1.51×10^{-1}	—	—
4	1.01	1.87	1.02	1.51×10^{-1}	-6.08×10^{-2}	—
5	1.01	1.91	1.02	1.04×10^{-1}	-6.08×10^{-2}	7.45×10^{-3}

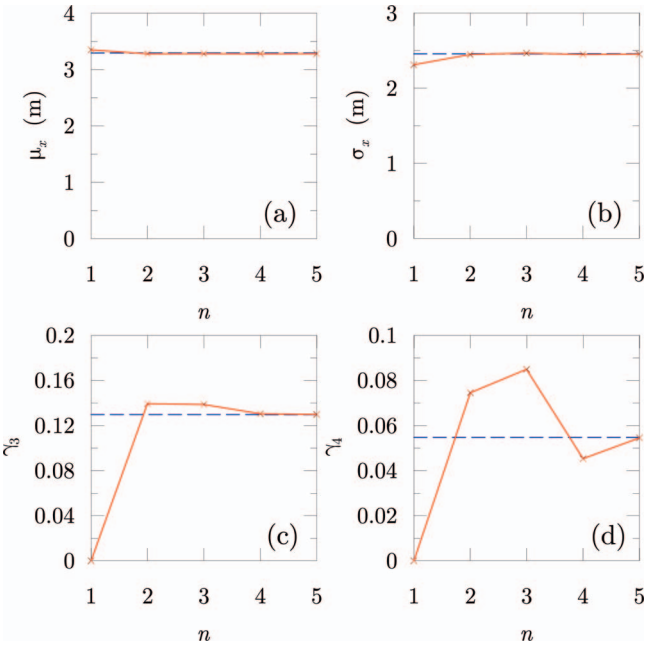

Fig. 17. (Color) Example 4: mean (a); SD (b); skewness (c); and COE (d) of the response by nth-order Volterra series ($\times$) and time-domain MCS (dashed line)

the response statistics is performed by a MCS-based quadrature scheme while the time-domain MCS involves a total simulation length of about 1.3×10^7 s.

Fig.17 shows the mean (a), SD (b), skewness (c), and COE (d) of the response x obtained setting the order of the Volterra operator $\mathcal{H}$, as well as the order of the polynomial approximation of the viscous term to $n=1$ to 5. The results of the time-domain MCS are reported with dashed lines and the coefficients a_r employed in the polynomial approximations are reported in Table 3. The accurate approximation of mean and SD is achieved by $n=2$ while the correct estimation of skewness and COE needs $n=4$ and $n=5$, respectively. It should be noted, however, that both skewness and COE are quite close to 0, thus the errors involved in the approximations are numerically small.

Fig.18 shows the PSD of the response calculated by the time-domain MCS and by Volterra models with order $n=1$ to 5. The first-order model matches the target PSD in the range of the wave excitation (roughly $\omega>0.2$ rad/s), but it is inadequate to predict the so-called slow-drift component of the response [e.g., Choi et al. (1985) and Kareem and Li (1994)]. The PSD provided by the second- and third-order models matches quite well with the results of the time-domain MCS; a slight overestimation of the PSD in the very low-frequency range and at the resonance frequency is corrected by the fourth- and fifth-order terms of the series (frame in Fig. 18).

Fig. 19 compares the PDF of the response computed by the time-domain MCS and by Volterra models with order $n=1$ to 5. All the plots are nondimensionalized by the SD and centered at the mean evaluated by MCS. The probability distribution is almost Gaussian due to the circumstance that, in the present example, the inertial term of the Morrison equation dominates. A second-order Volterra model is sufficient to match the target PDF while the higher-order terms provide very small corrections.

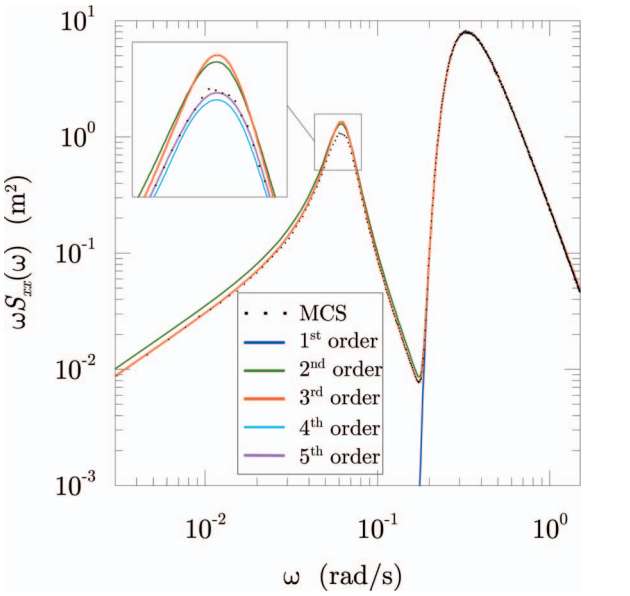

Fig. 18. (Color) Example 4: PSD of the response by time-domain MCS and Volterra models with order $n=1$ to 5

Example 5: Multiplicative Nonlinearity

In Examples 3 and 4, the wave action is idealized as acting at a single point of the structure located at the MWL. In reality, the hydrodynamic force is distributed along all the immersed structural members and is variable according to the wave surface profile. It is clear that, discretizing the structural members by a finite element approach, the load acting on each node of the model can be represented by a force model similar to the ones adopted in Eq. (66) or (75), in which $u(t)$ represents the water particle velocity at the node location. In the neighborhood of the MWL, however, there are parts of the structure referred to as splash zone where

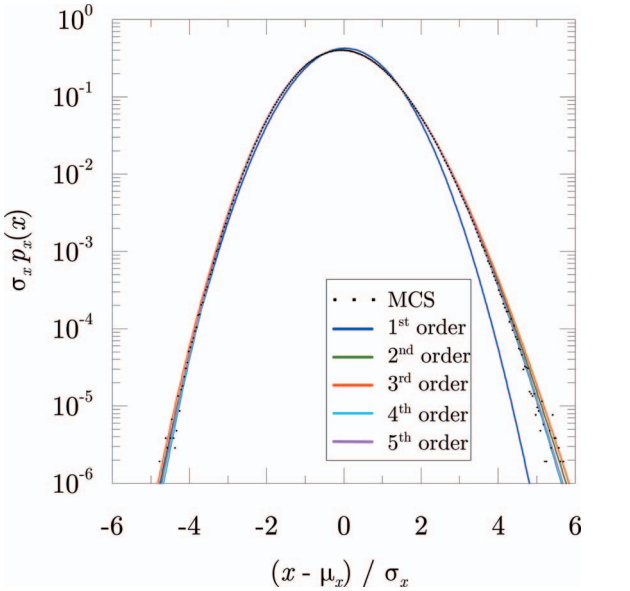

Fig. 19. (Color) Example 4: PDF of the response by the time-domain MCS and Volterra models with order $n=1$ to 5, nondimensionalized by the SD, and centered at the mean value obtained by MCS

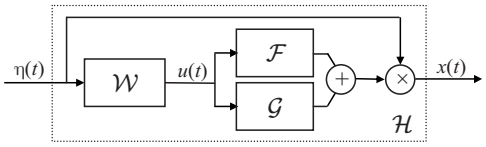

Fig. 20. Example 5: block diagram for Eq. (79)

the mentioned model cannot be directly applied since the wave-induced force is intermittent due to the variable wetted surface.

The wave-induced force in the splash zone can be modeled considering two contributions: a term representing the force acting below the MWL, modeled according to the standard Morison equation, and a term representing the correction necessary to take into account the variable wetted surface. This latter term can be expressed as (Li and Kareem 1993):

$$x(t) = \eta(t)\{k_d|U + u(t)|[U + u(t)] + k_m\dot{u}(t)\} \tag{79}$$

and contains a multiplicative nonlinearity due to the product between the wave elevation η and the Morison-type force.

In this example, only the above mentioned corrective term is considered and modeled by a Volterra series. In practical applications, this term should be added to the standard Morison equation and used as a force acting on the structure. This operation is straightforward using the assemblage rules defined in the Evaluation of the VFRFs Section.

The system defined by Eq. (79) can be translated into the block diagram shown in Fig. 20, in which the operators $\mathcal{F}$ and $\mathcal{G}$ have been defined by Eqs. (70), while $\mathcal{W}$ is the linear operator that provides $u(t)$ at the MWL given $\eta(t)$ which for deep water is defined by the FRF [e.g., Young (1999)]

$$W(\omega) = |\omega| \tag{80}$$

The VFRFs of the whole system $\mathcal{H}$ providing the correction to the force in the splash zone, given the wave elevation η, can be derived applying the rules for the sum [Eq. (26)], the product [Eq. (31)] and the series combination [Eq. (45)] of Volterra systems, resulting to $H_0=0$

$$H_1(\omega) = k_d a_0$$

$$H_2(\omega_1,\omega_2) = (k_d a_1 + i\omega_1 k_m)|\omega_1|$$

$$H_j(\mathbf{\Omega}_j) = k_d a_{j-1}\prod_{r=1}^{j-1}|\omega_r| \quad j \geq 3 \tag{81}$$

where a_r=coefficients deriving from the polynomial approximation of the operator $\mathcal{G}$.

The numerical example is developed considering the same numerical data as in Example 3 with the exception of $k_d=8.1\times10^3$ kg/m^2 and $k_m=4.8\times10^5$ kg/m. The approximation coefficients a_k are given in Table 2. The integration of the VFRFs was performed by an MCS-based quadrature scheme while the time-domain MCS involved a total simulation length of about 6.5×10^5 s.

Fig. 21 shows the mean (a), SD (b), skewness (c), and COE (d) evaluated by integrating [through Eq. (51)] the VFRFs given by Eqs. (81) up to the order $n=1$ to 5. It can be observed that mean, SD, and COE are correctly approximated by a second-order Volterra series while the accurate estimation of the skewness requires a fourth-order model. It is worth noting that the first-order term does not provide any significant contribution to the response.

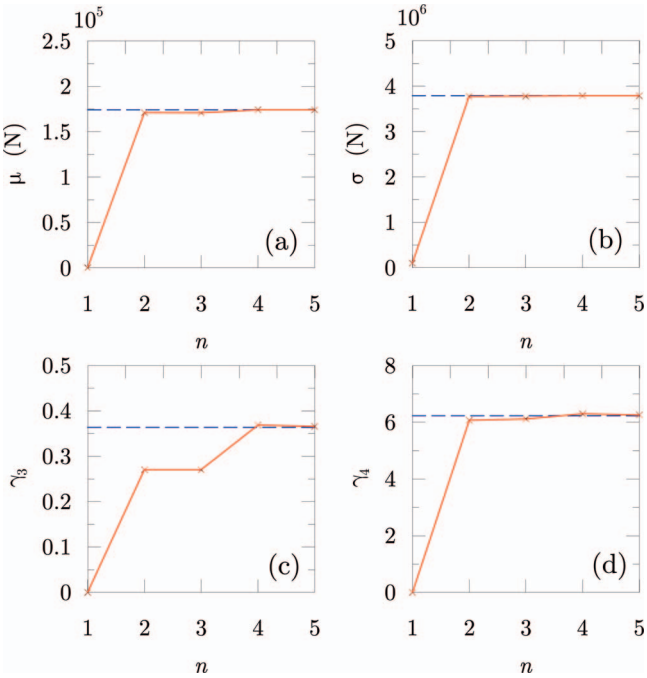

Fig. 21. (Color) Example 5: mean (a); SD (b); skewness (c); and COE (d) of the wave-force corrective term by nth-order Volterra series (×) and time-domain MCS (dashed line)

Fig. 22 compares the PSD of the splash-zone force correction term calculated by the time-domain MCS and by Volterra models with order $n=1$ to 4 (the fifth-order term does not provide any notable contribution to the PSD). The PSD obtained by the second-order Volterra model is quite accurate and the corrections introduced by the third- and fourth-order terms are very small.

Fig. 23 compares the PDF evaluated by time-domain MCS and by Volterra models with order $n=2$ to 4. The result of the first-order model has been omitted since it is not significant (as re-

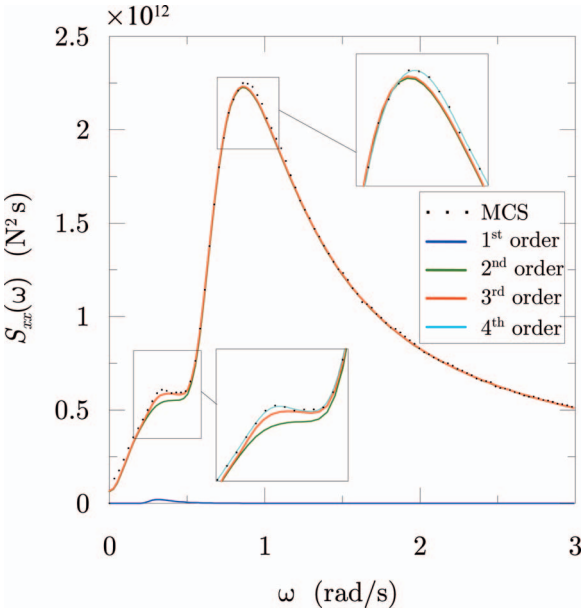

Fig. 22. (Color) Example 5: PSD of the wave-force corrective term by time-domain MCS and Volterra models with order $n=1$ to 4

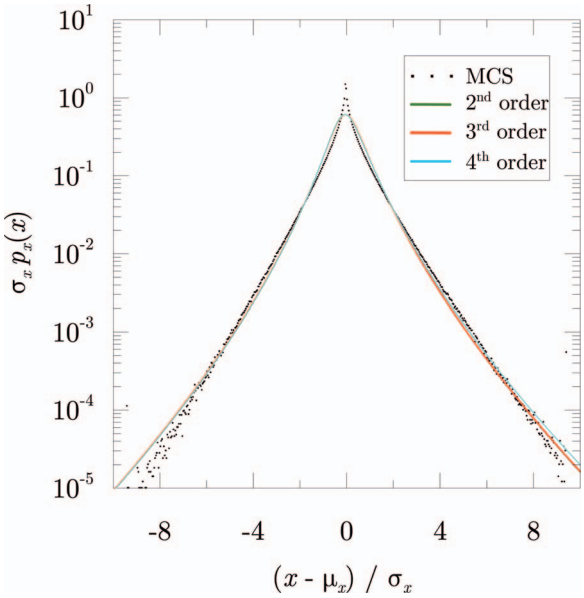

Fig. 23. (Color) Example 5: PDF of the wave-force corrective term by the time-domain MCS and Volterra models with order $n=2$ to 4, nondimensionalized by the SD, and centered at the mean value obtained by MCS

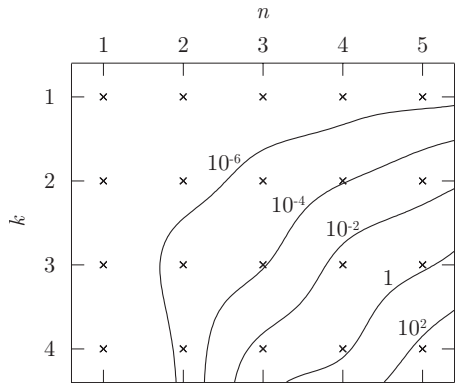

Fig. 24. Ratio between the computational times required for the evaluation of the kth-order statistical moment of an nth-order Volterra series and the time-domain MCS

ported in Fig. 21, its SD is only a small fraction of the actual SD), while the PDF obtained through the fifth-order model have not been reported since the fifth-order term of the series does not provide any notable modification to the PDF. The PDF obtained by the second-order model is coincident with the plot referred to the third-order model. The plots are nondimensionalized by the SD and centered at the mean value obtained by the MCS.

Discussion

The numerical examples presented in the preceding section demonstrate the versatility of the proposed method for the identification of the VFRFs of dynamical systems characterized by different assemblage topologies. Two features, though related with the application of the proposed technique, have not been treated here as despite their relative significance are not the central theme of this study, i.e., to provide an effective alternative to the harmonic probing scheme for modeling of complex systems.

The first feature concerns the convergence of the Volterra series used here to represent a given dynamical system. The Volterra series may be viewed as a generalization of the Taylor power series and, as such, it inherits its convergence-related issues. In particular, it is well known that the convergence of the Volterra series is assured only within a specific range of the input excitation amplitude referred to as region of convergence. Such a region can be estimated through a parametric analysis or, in very special cases, by analytical approaches [e.g., Worden et al. (1997)]. As far as the examples presented here are concerned, it can be demonstrated that the Volterra series employed in Examples 1, 3, and 5 are convergent for any amplitude of the respective inputs. In the case of Examples 2 and 4, the convergence of the series is only demonstrated by a parametric study, carried out by the writers, involving a large parameter space. It is difficult to establish a general metric of the reliability of the current approach as such a measure is quite problem-specific and even a very extensive parametric study may not be able to distinctly delineate domains of convergence.

The second feature is related to the computational complexity involved in the evaluation of the response statistics through the integration of the VFRFs. From the inspection of (51) it could be noted that the dimension of the integration domain increases both as the order n of the Volterra series and the order k of the statistical moment to be evaluated increase. Such a dimension, however, cannot be readily evaluated form Eq. (51) since, due to the symmetric nature of the VFRFs, the integral can be often factorized.

As a simple indicator of the computational time required to evaluate such integrals, Fig. 24 shows the time necessary to evaluate the kth-order statistical moment of the output of an nth-order Volterra system (for $k=1$ to 4 and $n=1$ to 5) divided by the time required by the time-domain MCS, referring to in the case of Example 4. The results, represented by a contour plot, show that for low-order Volterra series and low-order statistical moments the integration of the VFRFs is much faster than the time-domain MCS. The evaluation of the skewness of a fifth-order Volterra system or the evaluation of the COE of a fourth-order Volterra system requires time comparable to the time-domain MCS. However, the evaluation of the COE of a fifth-order Volterra system requires about 100 times longer than the time-domain MCS.

These results are just a simple representation of the relative efficiency of the Volterra-based analysis and the MCS since other problem-specific issues such as computer used, numerical integration scheme and subjective choice of the number of samples in the MCS scheme play an important role. Besides, it should be mentioned that the computational complexity of the procedure for the evaluation of the statistical moments can be significantly reduced for particular classes of Volterra systems as shown in Spanos et al. (2003) and that the time required by the time-domain MCS can be notably increased when the dynamical system does not have a differential form, e.g., dynamical systems with frequency-dependent parameters or systems that are partially defined by Volterra operators identified from experimental data.

Conclusions

The modeling of a given dynamical system as an assemblage of elementary building-block operators enables the evaluation of its

VFRFs of any order by means of algebraic rules that can be easily implemented into a symbolic-calculus computer code. In the case of Gaussian input, the use of such assemblage rules provides the expression for the statistical moments (of any order) of the response. These expressions are simplified so that they can be implemented into numerical routines to evaluate the statistical moments by conventional or MCS-based quadrature methods. This facilitated evaluation of the fifth-order Volterra models for the first time in the literature. In the proposed examples the third-order models provided reasonably accurate results as far as the PSD was concerned, however, the contribution of the fourth- and fifth-order terms of the series were needed for the higher-order statistics, e.g., skewness and kurtosis.

The proposed framework for the evaluation of VFRFs, besides being much simpler than the traditional harmonic probing, can treat cases in which a combination of analytical and experimental models exist and can be immediately extended to analyze multidegree-of-freedom systems for which the traditional methods become very challenging and often computationally prohibitive (Worden et al. 1997).

Acknowledgments

The funding for this work was provided in part by a grant from NSF (Grant No. CMMI0928282).

Appendix. Expanded Version of Some Equations

In this Appendix, expanded versions of some equations reported in the paper in a compact form are provided.

Expanded version of Eq. (3) for the orders $j=1$ to 3

$$\mathcal{H}_1[u(t)] = \int_{-\infty}^{\infty} h_1(\tau_1)u(t-\tau_1)d\tau_1$$

$$\mathcal{H}_2[u(t)] = \int_{-\infty}^{\infty}\int_{-\infty}^{\infty} h_2(\tau_1,\tau_2)u(t-\tau_1)u(t-\tau_2)d\tau_1 d\tau_2$$

$$\mathcal{H}_3[u(t)] = \int_{-\infty}^{\infty}\int_{-\infty}^{\infty}\int_{-\infty}^{\infty} h_3(\tau_1,\tau_2,\tau_3)u(t-\tau_1)u(t-\tau_2) \times u(t-\tau_3)d\tau_1 d\tau_2 d\tau_3 \quad (82)$$

Expanded version of Eq. (12) for the orders $j=1$ to 3

$$\mathcal{H}_1[u(t)] = \int_{-\infty}^{\infty} e^{i\omega t}H_1(\omega)dU(\omega)$$

$$\mathcal{H}_2[u(t)] = \int_{-\infty}^{\infty}\int_{-\infty}^{\infty} e^{i(\omega_1+\omega_2)t}H_2(\omega_1,\omega_2)dU(\omega_1)dU(\omega_2)$$

$$\mathcal{H}_3[u(t)] = \int_{-\infty}^{\infty}\int_{-\infty}^{\infty}\int_{-\infty}^{\infty} e^{i(\omega_1+\omega_2+\omega_3)t}H_3(\omega_1,\omega_2,\omega_3)dU(\omega_1) \times dU(\omega_2)dU(\omega_3) \quad (83)$$

Expanded version of Eq. (13) for the orders $j=1$ to 3

$$dX_1(\omega) = H_1(\omega)dU(\omega)$$

$$dX_2(\omega) = \int_{-\infty}^{\infty} H_2(\omega_1,\omega-\omega_1)dU(\omega_1)dU(\omega-\omega_1)$$

$$dX_3(\omega) = \int_{-\infty}^{\infty}\int_{-\infty}^{\infty} H_3(\omega_1,\omega_2,\omega-\omega_1-\omega_2)dU(\omega_1)dU(\omega_2) \times dU(\omega-\omega_1-\omega_2) \quad (84)$$

Expanded version of Eq. (31) for $j=0$ to 3

$$H_0 = A_0B_0$$

$$H_1(\omega) = A_0B_1(\omega) + A_1(\omega)B_0$$

$$H_2(\omega_1,\omega_2) = A_0B_2(\omega_1,\omega_2) + A_1(\omega_1)B_1(\omega_2) + A_2(\omega_1,\omega_2)B_0$$

$$H_3(\omega_1,\omega_2,\omega_3) = A_0B_3(\omega_1,\omega_2,\omega_3) + A_1(\omega_1)B_2(\omega_2,\omega_3) + A_2(\omega_1,\omega_2)B_1(\omega_3) + A_3(\omega_1,\omega_2,\omega_3)B_0 \quad (85)$$

Expanded version of Eq. (41) with $n_B=3$, for the orders $j=1$ to 3, plus $\alpha_p^{(j,k)}$ terms used in the generation

$$\begin{aligned} H_1(\omega) &= B_1(\omega)A_1(\omega) \quad (\alpha_p^{(1,1)} = 1) \\ &+ 2B_2(0,\omega)A_0A_1(\omega) \quad (\alpha_p^{(1,2)} = 0,1) \\ &+ 3B_3(0,0,\omega)A_0^2A_1(\omega) \quad (\alpha_p^{(1,3)} = 0,0,1) \end{aligned}$$

$$\begin{aligned} H_2(\omega_1,\omega_2) &= B_1(\omega_1+\omega_2)A_2(\omega_1,\omega_2) \quad (\alpha_p^{(2,1)} = 2) \\ &+ B_2(\omega_1,\omega_2)A_1(\omega_1)A_1(\omega_2) \quad (\alpha_p^{(2,2)} = 1,1) \\ &+ 2B_2(0,\omega_1+\omega_2)A_0A_2(\omega_1,\omega_2) \quad (\alpha_p^{(2,2)} = 0,2) \\ &+ 3B_3(0,0,\omega_1+\omega_2)A_0^2A_2(\omega_1,\omega_2) \quad (\alpha_p^{(2,3)} = 0,0,2) \\ &+ 3B_3(0,\omega_1,\omega_2)A_0A_1(\omega_1)A_1(\omega_2) \quad (\alpha_p^{(2,3)} = 0,1,1) \end{aligned}$$

$$\begin{aligned} H_3(\omega_1,\omega_2,\omega_3) &= B_1(\omega_1+\omega_2+\omega_3)A_3(\omega_1,\omega_2,\omega_3) \quad (\alpha_p^{(3,1)} = 3) \\ &+ 2B_2(0,\omega_1+\omega_2+\omega_3)A_0A_3(\omega_1,\omega_2,\omega_3) \quad (\alpha_p^{(3,2)} = 0,3) \\ &+ 2B_2(\omega_1,\omega_2+\omega_3)A_1(\omega_1)A_2(\omega_2,\omega_3) \quad (\alpha_p^{(3,2)} = 1,2) \\ &+ B_3(\omega_1,\omega_2,\omega_3)A_1(\omega_1)A_2(\omega_2)A_3(\omega_3) \quad (\alpha_p^{(3,3)} = 1,1,1) \\ &+ 3B_3(0,0,\omega_1+\omega_2+\omega_3)A_0^2A_3(\omega_1,\omega_2,\omega_3) \quad (\alpha_p^{(3,3)} = 0,0,3) \\ &+ 6B_3(0,\omega_1,\omega_2+\omega_3)A_0A_1(\omega_1)A_2(\omega_2,\omega_3) \quad (\alpha_p^{(3,3)} = 0,1,2) \end{aligned} \quad (86)$$

Expanded version of Eq. (50) for $n=4$

$$E(\mathcal{H}[u]) = H_0 + \int_{-\infty}^{\infty} H_2(\omega,-\omega)S_{uu}(\omega)d\omega + 3\int_{-\infty}^{\infty}\int_{-\infty}^{\infty} H_4(\omega_1,\omega_2,-\omega_1, -\omega_2)S_{uu}(\omega_1)S_{uu}(\omega_2)d\omega_1 d\omega_2 \quad (87)$$

Expanded version of Eq. (51) for $k=2$ and $n=3$

$$
\begin{aligned}
m_2(\mathcal{H}[u]) &= H_0^2 && (\alpha_p^{(0,2)} = 0,0)\\
&+ 2H_0 \int_{\mathbb{R}} H_2(\omega,-\omega) S_{uu}(\omega) d\omega && (\alpha_p^{(2,2)} = 0,2)\\
&+ \int_{\mathbb{R}} |H_1(\omega)|^2 S_{uu}(\omega) d\omega && (\alpha_p^{(2,2)} = 1,1)\\
&+ 6 \int_{\mathbb{R}^2} H_1(\omega_1) H_3(-\omega_1,\omega_2,-\omega_2) \prod_{r=1}^{2} S_{uu}(\omega_r) d\omega_r && (\alpha_p^{(4,2)} = 1,3)\\
&+ 2 \int_{\mathbb{R}^2} |H_2(\omega_1,\omega_2)|^2 \prod_{r=1}^{2} S_{uu}(\omega_r) d\omega_r\\
&+ \int_{\mathbb{R}^2} H_2(\omega_1,-\omega_1) H_2(\omega_2,-\omega_2) \prod_{r=1}^{2} S_{uu}(\omega_r) d\omega_r && (\alpha_p^{(4,2)} = 2,2)\\
&+ 6 \int_{\mathbb{R}^3} |H_3(\omega_1,\omega_2,\omega_3)|^2 \prod_{r=1}^{3} S_{uu}(\omega_r) d\omega_r\\
&+ 9 \int_{\mathbb{R}^3} H_3(\omega_1,-\omega_1,\omega_2) H_3(-\omega_2,\omega_3,-\omega_3) && (\alpha_p^{(6,2)} = 3,3)\\
&\times \prod_{r=1}^{3} S_{uu}(\omega_r) d\omega_r
\end{aligned}
\tag{88}
$$

It can be observed that some of the terms present in Eq. (88) (namely, terms 1, 2, and 6) can be factorized. Similar terms are also present in the expressions of high-order moments and correspond to products of lower-order moments $\{m_1[\mathcal{H}]^2$ in the case of Eq. (88)$\}$. Expressions for the cumulants can be obtained removing the factorized terms from the expression of the corresponding statistical moments [e.g., the variance is obtained from Eq. (88) by eliminating the first, second, and sixth terms).

The expression for the output PSD of a third-order Volterra series is given by

$$
\begin{aligned}
S_{xx}(\omega) &= E[x]^2 \delta(\omega) + |H_1(\omega)|^2 S_{uu}(\omega)\\
&+ 6 S_{uu}(\omega) \int_{\mathbb{R}} H_1(\omega) H_3(-\omega,\omega_1,-\omega_1) S_{uu}(\omega_1) d\omega_1\\
&+ 2 \int_{\mathbb{R}} |H_2(\omega_1,\omega-\omega_1)|^2 S_{uu}(\omega_1) S_{uu}(\omega-\omega_1) d\omega_1\\
&+ 6 \int_{\mathbb{R}^2} |H_3(\omega_1,\omega_2,\omega-\omega_1-\omega_2)|^2\\
&\times S_{uu}(\omega_1) S_{uu}(\omega_2) S_{uu}(\omega-\omega_1-\omega_2) d\omega_1 d\omega_2\\
&+ 9 S_{uu}(\omega) \int_{\mathbb{R}^2} H_3(\omega,\omega_1,-\omega_1) H_3(-\omega,\omega_2,\\
&- \omega_2) S_{uu}(\omega_1) S_{uu}(\omega_2) d\omega_1 d\omega_2
\end{aligned}
\tag{89}
$$

References

Amblard, P. O., Gaeta, M., and Lacoume, J. L. (1996). "Statistics for complex random variables and signals. Part I: Variables." *Signal Process.*, 53, 1–13.

Bedrosian, E., and Rice, S. O. (1971). "The output of Volterra systems (nonlinear systems with memory) driven by harmonic and Gaussian inputs." *Proc. IEEE*, 59(12), 1688–1707.

Carassale, L., and Karrem, A. (2003). "Dynamic analysis of complex nonlinear systems by Volterra approach." *Proc., Computational Stochastic Mechanics, CSM4*, P. D. Spanos and G. Deodatis, eds., Millipress, Rotterdam, The Netherlands, 107–117.

Carassale, L., and Solari, G. (2006). "Monte Carlo simulation of wind velocity fields on complex structures." *J. Wind Eng. Ind. Aerodyn.*, 94, 323–339.

Chakrabarti, S. K. (1990). *Nonlinear methods in offshore engineering*, Elsevier, Amsterdam.

Choi, D., Miksad, R. W., and Powers, E. J. (1985). "Application of digital cross-bispectral analysis techniques to model the non-linear response of a moored vessel system in random seas." *J. Sound Vib.*, 99(3), 309–326.

Donley, M. G., and Spanos, P. D. (1990). *Dymanic analysis of non-linear structures by the method of statistical quadratization*, Springer, New York.

Donley, M. G., and Spanos, P. D. (1991). "Stochastic response of a tension leg platform to viscous drift forces." *J. Offshore Mech. Arct. Eng.*, 113(2), 148–155.

Grigoriu, M. (1984). "Crossings of non-Gaussian translation processes." *J. Eng. Mech.*, 110(4), 610–620.

Kareem, A., and Li, Y. (1994). "Stochastic response of a tension leg platform to viscous and potential drift forces." *Probab. Eng. Mech.*, 9(1–2), 1–14.

Kareem, A., Williams, A. N., and Hsieh, C. C. (1994). "Diffraction of nonlinear random waves by a vertical cylinder in deep water." *Ocean Eng.*, 21(2), 129–154.

Kareem, A., Zhao, J., and Tognarelli, M. A. (1995). "Surge response statistics of tension leg platforms under wind & wave loads: a statistical quadratization approach." *Probab. Eng. Mech.*, 10(4), 225–240.

Koukoulas, P., and Kalouptsidis, N. (1995). "Nonlinear system identification using Gaussian inputs." *IEEE Trans. Signal Process.*, 43, 1831–1841.

Li, X. M., Quek, S. T., and Koh, C. G. (1995). "Stochastic response of offshore platforms by statistical cubicization." *J. Eng. Mech.*, 121(10), 1056–1068.

Li, Y., and Kareem, A. (1993). "Multivariate Hermite expansion of hydrodynamic drag loads on tension leg platforms." *J. Eng. Mech.*, 119(1), 91–112.

Lucia, D. J., Beranb, P. S., and Silva, W. A. (2004). "Reduced-order modeling: New approaches for computational physics." *Prog. Aerosp. Sci.*, 40, 51–117.

Peyton Jones, J. C. (2007). "Simplified computation of the Volterra frequency response functions of non-linear systems." *Mech. Syst. Signal Process.*, 21, 1452–1468.

Priestley, M. B. (1981). *Spectral analysis and time series*, Academic, San Diego.

Schetzen, M. (1980). *The Volterra and Weiner theories of nonlinear systems*, Wiley, New York.

Silva, W. (2005). "Identification of nonlinear aeroelastic systems based on the Volterra theory: progress and opportunities." *Nonlinear Dyn.*, 39, 25–62.

Solari, G., and Piccardo, G. (2001). "Probabilistic 3-D turbulence modeling for gust buffeting of structures." *Probab. Eng. Mech.*, 16, 73–86.

Spanos, P. D. and Donley, M. G. (1991). "Equivalent statistical quadratization for nonlinear systems." *J. Eng. Mech.*, 117(6), 1289–1310.

Spanos, P. D., and Donley, M. G. (1992). "Non-linear multi-degree-of-freedom system random vibration by equivalent statistical quadratization." *Int. J. Non-Linear Mech.*, 27(5), 735–748.

Spanos, P. D., Failla, G., and Di Paola, M. (2003). "Spectral approach to equivalent statistical quadratization and cubicization methods for nonlinear oscillators." *J. Eng Mech.*, 129(1), 31–42.

Tognarelli, M., and Kareem, A. (2001). "Equivalent cubicization for nonlinear systems." *Proc. 8th Int. Conf. on Structural Safety and Reliability, ICOSSAR* (CD-ROM), Lisse, Balkema, The Netherlands.

Tognarelli, M. A., Zhao, J., and Kareem, A. (1997b). "Equivalent statis-

tical cubicization for force and system nonlinearities." *J. Eng. Mech.*, 123(8), 890–893.
Tognarelli, M. A., Zhao, J., Rao, K. < middlename>B., and Kareem, A. (1997a). "Equivalent statistical quadratization and cubicization for nonlinear systems." *J. Eng Mech.*, 123(5), 512–523.
Volterra, V. (2005). "Theory of functionals and of integral and integrodifferential equations." Dover, New York.
Winterstein, S. R. (1985). "Non-normal response and fatigue damage." *J. Eng. Mech.*, 111(10), 1291–1295.
Winterstein, S. R. (1988). "Nonlinear vibration models for extremes and fatigue." *J. Eng. Mech.*, 114(10), 1772–1790.
Worden, K., and Manson, G. (2005). "A Volterra series approximation to the coherence of the Duffing oscillator." *J. Sound Vib.*, 286, 529–547.
Worden, K., Manson, G., and Tomlinson, G. R. (1997). "A harmonic probing algorithm for the multi-input Volterra series." *J. Sound Vib.*, 201(1), 67–84.
Young, I. R. (1999). *Wind generated ocean waves*, Elsevier, Oxford.